NRC Research Press

ARTICLE

Simulated instream restoration structures offer smallmouth bass (*Micropterus dolomieu*) swimming and energetic advantages at high flow velocities

Katherine K. Strailey, Ryan T. Osborn, Rafael O. Tinoco, Piotr Cienciala, Bruce L. Rhoads, and Cory D. Suski

Abstract: Restoration practices aimed at fish habitat enhancement often include installation of instream structures. However, mixed outcomes have been reported regarding structure effectiveness, while mechanisms underlying success remain unclear. The interactions between fish and flow conditions generated by instream structures and their subsequent impact on fish energetics may provide some insight. This study seeks to quantify how restoration structures, simulated by cylinders in three orientations, alter the energetics and swimming stability of smallmouth bass (*Micropterus dolomieu*). Accelerometers measured swimming stability while a respirometer measured energy expenditure at multiple velocities. Particle image velocimetry was used to characterize flow fields behind structures. Structures generated flow conditions that benefited fish energetically. Fish had a smoother gait and expended less energy when swimming near a structure, regardless of its orientation. Benefits varied with flow conditions; reductions in energy expenditure were especially apparent at high flow velocities. Results suggest that restoration structures may be most energetically beneficial in stream systems with consistently high velocities and inform restoration by indicating flow conditions in which structures provide the greatest energetic benefits for fish.

Résumé : Les pratiques de restauration visant à améliorer les habitats de poissons comprennent souvent l'aménagement d'ouvrages dans les cours d'eau. Des résultats mitigés ont toutefois été rapportés quant à l'efficacité de tels ouvrages, et les mécanismes qui sous-tendent cette dernière demeurent mal compris. Les interactions entre les poissons et les conditions d'écoulement produites par les ouvrages dans les cours d'eau et leur incidence subséquente sur l'énergétique des poissons pourraient fournir des indices. L'étude tente de quantifier comment des ouvrages de restauration, simulés par des cylindres de trois orientations différentes, modifient l'énergétique et la stabilité de nage d'achigans à petite bouche (*Micropterus dolomieu*). Des accéléromètres sont utilisés pour mesurer la stabilité de nage et un respiromètre, pour mesurer la dépense énergétique à différentes vitesses. La vélocimétrie par images de particules est utilisée pour caractériser les champs d'écoulement en arrière des ouvrages. Ces derniers produisent des conditions d'écoulement avantageuses pour les poissons sur le plan énergétique. Les poissons nagent de manière plus stable et dépensent moins d'énergie à proximité d'un ouvrage, peu importe son orientation. Les avantages varient selon les conditions d'écoulement; des réductions de la dépense énergétique sont particulièrement évidentes à de hautes vitesses d'écoulement. Les résultats portent à croire que les ouvrages de restauration pourraient offrir les plus grands avantages sur le plan énergétique dans les réseaux hydrographiques caractérisés par des vitesses d'écoulement uniformément élevées, et fournissent des renseignements utiles pour la restauration en indiquant les conditions d'écoulement dans lesquelles ces ouvrages offrent aux poissons les plus grands avantages énergétiques. [Traduit par la Rédaction]

Introduction

Freshwater ecosystems worldwide are currently at risk due to anthropogenic degradation that imperils water quality, connectivity, and biodiversity (Gleick 2003; Dudgeon et al. 2006; Vörösmarty et al. 2010). The United States Environmental Protection Agency (EPA) estimates that, of 750 000 sampled river kilometres in the United States, half were considered impaired, and nearly half (46%) were in poor biological condition (EPA 2017). In addition, between 10 000 and 20 000 freshwater species are at risk of extinction, and in North America, it is estimated that 39% of freshwater and diadromous fish species are imperiled (Jelks et al. 2008). Overall, freshwater systems are highly degraded, and the consequences of human impact are widespread.

Restoration is one way to counteract and mitigate the deterioration of fresh waters while complementing other conservation and management actions, such as erosion control, stormwater management, and riparian revegetation (Wohl et al. 2005, 2015; Bernhardt and Palmer 2007; Beechie et al. 2010). In the United States, tens of thousands of restoration projects have been undertaken over the past several decades, and this approach to stream management is now a multibillion dollar industry (Bernhardt

K.K. Strailey. Program in Ecology, Evolution, and Conservation Biology, University of Illinois at Urbana-Champaign, Urbana, IL 61801, USA.

R.T. Osborn. Department of Civil and Environmental Engineering, Virginia Polytechnic Institute and State University, Blacksburg, VA 24061, USA.

R.O. Tinoco. Department of Civil and Environmental Engineering, University of Illinois at Urbana-Champaign, Urbana, IL 61801, USA.

P. Cienciala, and B.L. Rhoads. Department of Geography and Geographic Information Science, University of Illinois at Urbana-Champaign, Urbana, IL 61801, USA.

C.D. Suski. Department of Natural Resources and Environmental Sciences, University of Illinois at Urbana-Champaign, Urbana, IL 61801, USA.

Corresponding author: Katherine K. Strailey (email: ks26@illinois.edu).

et al. 2005). The goals of river restoration vary widely, but generally focus on enhancing the environmental quality of human-impacted streams (Bernhardt et al. 2005). From an ecological perspective, restoration and the related activity of stream naturalization (Wade et al. 2002; Rhoads et al. 2011) often seek to counteract adverse impacts on aquatic communities through improvement of instream habitat (Bernhardt et al. 2005).

Many restoration efforts aimed at reversing declines in fish populations involve placement of artificial structures in streams or adoption of management approaches that encourage the development of natural structures in streams to improve physical habitat (Thompson 2006; Palmer et al. 2014). Artificial structures can be large and highly complex, such as engineered logjams and woody debris (Abbe and Brooks 2011), or small and simple, such as sunken root wads and lunkers (crib-like structures supported by vertical piles and sunken into banks to provide cover for fish; Radspinner et al. 2010). Besides providing habitat for fish, natural and artificial structures can also contribute to erosion control and flood protection (Gilvear et al. 2013). Structures can positively impact individual fish as well as fish populations and communities by increasing habitat heterogeneity (Tews et al. 2004), providing cover from predators (Fausch 1993), and generating regions of low-velocity flow that may benefit fish energetically (McMahon and Hartman 1989; Shuler et al. 1994; Antón et al. 2011; Boavida et al. 2011). As such, artificial instream structures as well as management approaches aimed at developing and preserving natural structures have been implemented widely to address a variety of issues related to degradation of the environmental quality of rivers (Nagayama and Nakamura 2010).

Despite widespread adoption of restoration strategies based on enhancement of instream structure through augmentation with artificial structures or promotion of natural structure development, mixed outcomes have been reported, with not all projects resulting in enhancements to fish populations (Kail et al. 2015). In fact, many restoration projects intended to increase fish population size and biodiversity through improved habitat heterogeneity have been ineffective (Stewart et al. 2009; Palmer et al. 2010; Lepori et al. 2005). Long-term impacts of instream structures on population changes often are difficult to assess because few projects include pre- and postproject monitoring (Downs and Kondolf 2002; Bernhardt et al. 2007). The response time to changes in habitat remains poorly constrained, and many years of monitoring may be required to determine whether instream habitat structures actually benefit fish populations (Louhi et al. 2016). Moreover, any favorable biological responses that are documented, such as increases in fish abundance or biomass, typically are assumed to result from restoration, yet detailed mechanism(s) underlying these changes remain unknown.

Stream restoration may yield inconsistent results, in part, due to a lack of understanding of the mechanisms that guide fish interactions with natural or artificial structures. The majority of studies examining restoration success have focused primarily on ecological metrics, such as changes in population size or community dynamics, that may be unable to clearly attribute responses to habitat enhancement. In contrast, physiological metrics, which can influence life history (Ricklefs and Wikelski 2002), community composition (Start et al. 2018), and species resilience (Hofmann and Todgham 2010), have largely been ignored. Individual physiology responds swiftly to changes in the environment and as such may contribute to a more holistic, mechanistic understanding of how restoration impacts fish.

The small-scale interactions between fish and structure-induced flow characteristics are rarely emphasized in either instream structure design or project monitoring; instead, the research, design, and evaluation of instream restoration structures largely focus on geomorphic effects, such as increased scour and pool formation and erosion-control benefits that

contribute to channel stability (Thompson 2002; Miller and Kochel 2010; Radspinner et al. 2010; Bennett et al. 2015). This is a concern because both natural obstructions and instream structures alter flow characteristics (Daniels and Rhoads 2013; Bennett et al. 2015), largely by generating coherent turbulent structures that increase levels of turbulence. Instream structure provides cover from predators and increases food availability (Angermeier and Karr 1984; Schneider and Winemiller 2008), but also generates turbulence that affects fish swimming behavior, kinematics, and energy consumption (Tritico and Cotel 2010; Tullos and Walter 2015; Maia et al. 2015). Turbulence in rivers is characterized by chaotic, irregular fluctuations in velocity imposed onto mean flow, manifesting as vortices and eddies of various sizes and strengths (Warhaft 2002). The size, orientation, and intensity of such turbulence features are dependent on the mean water velocity, the depth of flow, and the characteristics of instream structures (Williamson 1996; Beal et al. 2006), while the intensity, periodicity, orientation, and scale of turbulent eddies, along with fish size and shape (Lupandin 2005; Tritico and Cotel 2010), determine interactions between fish and turbulence (Lacey et al. 2012). High levels of turbulence may place a large energetic burden on fish, in turn affecting fish position choice and habitat selection (Wilkes et al. 2017). On the other hand, certain patterns of coherent fluid motion may correspond to patterns of swimming mechanics by fish, thereby conferring reducing energetic costs (Liao et al. 2003b; Taguchi and Liao 2011). The possible energetic benefits of instream structure may be increased if structures are able to generate such flow conditions. However, the interactions between fish and turbulence are generally understudied outside of a handful of species, and studies emphasizing turbulence generated by instream structures largely focus on large-scale turbulence (Tullos and Walter 2015; Tullos et al. 2016).

The goal of this study is to quantify the local interactions between a riverine fish and simulated instream structures immediately downstream from structures using an experimental, laboratory-based approach. We investigated the influence of structures on swimming performance and energetics and chose to focus on energetics because energy expenditure is a metric firmly based on well-understood physiological mechanisms, as well as being particularly sensitive to environmental conditions and can be immediately responsive to changes in the environment (Enders and Boisclair 2016), such as the altered flows and turbulence generated by instream structures. Fish were placed in a swimming respirometer outfitted with several different structures to vary flow conditions and explore potential influences of orientation or design elements of artificial structures. Rate-of-change accelerometers were implanted in fish to quantify position stability, concurrent with measurements of oxygen consumption; position stability was expected to decrease as water velocity increased, and fish increasingly became unstable swimming within the respirometer. Flow in the respirometer was characterized through the use of particle image velocimetry (PIV), with a particular emphasis on the intensity and orientation of turbulent vortices in addition to mean flow characteristics. The centrarchid smallmouth bass (*Micropterus dolomieu*) was selected as the model species for this study, as these river-dwelling fish often are a target species for instream restoration efforts in the United States (Moerke and Lamberti 2003; Hrodey and Sutton 2008). Results contribute to the understanding of fish energetics and provide insight into the physical characteristics of stream restoration structures that maximize energetic benefits for fish.

Methods

Fish collection and care

Smallmouth bass (*n* = 48) were delivered from Jake Wolf Memorial Fish Hatchery (Topeka, Illinois) to the Illinois Natural History Survey Aquatic Research Facility (Champaign, Illinois) on 21 September

Table 1. Average size of smallmouth bass, along with metrics of water quality data, across the 60-day acclimation period at one of three different temperature treatments.

Treatment temperature (°C)	Mean temperature (°C)	Total length (cm)	Mass (g)	Dissolved oxygen saturation (%)	Ammonia (ppm)
15	15.6 ($\pm$0.16)	29.7 ($\pm$0.5)	303.5 ($\pm$13.1)	93.2	<1.0
18	18.3 ($\pm$0.08)	29.5 ($\pm$0.6)	309.0 ($\pm$16.7)	94.3	<1.0
21	20.8 ($\pm$0.04)	30.1 ($\pm$0.3)	325.0 ($\pm$6.9)	91.9	<1.0

Note: Smallmouth bass were measured following the end of the acclimation period, while water quality metrics were measured either daily (temperature and dissolved oxygen saturation) or every several days (ammonia). Length and mass data are shown with standard error and did not vary across temperature treatments ($P > 0.05$).

2018. Upon arrival at the aquatic facility, smallmouth bass were held overnight in outdoor, 1135 L circular tanks to recover from hauling; tanks were connected to an earthen-bottom pond, and water temperature was 22 °C. The following day, each fish was weighed to the nearest gram (overall mean = 296.9 ± 11.3 g standard error, SE) and its total length (TL) measured to the nearest centimetre (mean = 27.5 ± 0.4 cm SE), before being divided among three indoor 567 L tanks at an initial temperature of 22 °C. Water temperature in these indoor tanks was then adjusted by 1 °C every day using heater–chiller units (TK 500, TECO, Ravenna, Italy) until treatment temperatures of 15, 18, and 21 °C were reached (Peake et al. 1997; Webb 1998); these temperatures reflect a range of ecologically relevant temperatures commonly encountered by stream-dwelling smallmouth bass (McClendon and Rabeni 1987; Wehrly et al. 2003). Multiple acclimation temperatures were utilized because swimming performance can vary across temperatures (Hocutt 1973; Kolok 1991), oxygen consumption (MO$_2$) correlates positively with temperature (Enders et al. 2003), and the use of multiple temperatures increases the range of temperatures at which conclusions could be drawn for wild, free-swimming smallmouth bass. Once target temperatures were reached, an acclimation period began, and fish remained at target temperatures for between 65 and 70 days to ensure thermal acclimation (Johnston and Dunn 1987; Currie et al. 1998; Sandblom et al. 2014). Throughout the acclimation period, water quality (levels of dissolved oxygen and ammonia) was measured regularly (YSI Inc. Professional Plus; API Ammonia Test Kit; Table 1). Smallmouth bass were fed live minnows (e.g., fathead minnows, *Pimephales promelas*) once a week at a rate of 2% of their body mass.

Tagging procedure

Following the end of the acclimation period, each smallmouth bass was surgically implanted with an accelerometer tag (model MCFT3-SO, 6.8 g in air, 12.5 Hz recording frequency; Lotek Wireless, Newmarket, Ontario, Canada) to quantify position stability during swim trials. These tags measured jerk acceleration (i.e., the rate of change of acceleration), which has previously been used to quantify position changes in other aquatic organisms, including Chinook salmon (*Oncorhynchus tshawytscha*) passing through dams and feeding harbor seal (*Phoca vitulina*) (Deng et al. 2005; Ydesen et al. 2014); jerk acceleration was utilized as fish become increasingly unstable as water velocity increases and they approach the point of fatigue (Beamish 1970; Webb 1971). On average, tag burden was 2.17% of body mass, and for the smallest individuals, the mass of the accelerometer tag in air did not exceed 4% body mass (Cooke et al. 2011). Visual inspections ensured that the volume of the tag was appropriate for the body cavity of the fish. Surgeries followed methods outlined in Wagner et al. (2011) and Harms (2005), and all fish were fasted for a minimum of 48 h before surgeries took place to allow sufficient time for digestion (Adams et al. 1998).

Fish were anesthetized with AQUI-S 10E (AQUI-S New Zealand LTE, Lower Hutt, New Zealand) at a concentration of 50 mg·L^{-1} at a temperature identical to their acclimation temperature, until they lost equilibrium and were unresponsive to tail pinches.

Each individual was then weighed, measured, and transferred to a wet surgical tray for tagging; no significant loss of mass was observed for the group as a whole between fish arrival at the facility and tagging (Welch two-sample t test, $t_{[83.9]} = -0.97$, $P = 0.34$). A tube was placed into the fish's mouth to provide a constant flow of AQUI-S 10E-dosed water over the gills and maintain anesthetization. A 15 mm long incision parallel to the ventral midline was made 2 mm anterior to the terminus of the pelvic fins and 1 mm off of the ventral midline. The accelerometer was gently inserted into the peritoneal cavity, while the antenna exited through the incision and was allowed to trail freely. The incision was then closed with a single absorbable suture (M452, size 3/0, NFS-2 needle; SouthPointe Surgical, Coral Springs, Florida), and fish were immediately placed in a container of aerated water, matched to their acclimation temperature, to facilitate recovery. Once equilibrium was regained and normal swimming behavior resumed, fish were transferred to isolation totes and returned to their original acclimation tank. Isolation totes were clear and allowed for water flow and visual contact with other fish but prevented physical interaction or tangling of antennas. Each fish was allowed to recover overnight for a minimum of 16 h after tagging before participating in respirometer swim trials (Wilson et al. 2013), and no more than 7 days passed between a fish's tagging event and its inclusion in swim trials (Rodgers et al. 2016; Svendsen et al. 2016). All surgeries were performed by the same individual, and mean surgery time was 3:53 min ($\pm$6.8 s SE).

Respirometer swim trials

Quantification of MO$_2$ (energy use) when interacting with simulated instream structures was performed with tagged fish in a 30 L Steffensen-type swimming respirometer (model number SW10150; Loligo Systems, Viborg, Denmark; Fig. 1a) using intermittent-flow respirometry (Steffensen et al. 1984; Nelson 2016; Svendsen et al. 2016). The manufacturer indicates that this swimming respirometer is ideally suited for fish weighing between 175 and 500 g (https://www.loligosystems.com/swim-tunnel-respirometer-3). Experimental treatments with turbulent flow consisted of the addition of a single 2.54 cm diameter clear acrylic cylinder (hereinafter referred to as a structure) securely mounted in the swimming chamber in one of three orientations (Taguchi and Liao 2011). In addition, control trials were conducted with no structures (NS). The reference frame is defined such that X is the longitudinal coordinate in the direction of the mean flow, Y is the horizontal transverse coordinate perpendicular to the mean flow, and Z is vertical (Figs. 1b–1f). The structure was thus aligned with the Y axis (horizontal structure, HS), Z axis (vertical structure, VS), and diagonally within the YZ plane (diagonal structure, DS). VS was placed on the centerline of the chamber, HS was centered at half depth, and DS was placed with the high end of the structure against the swim chamber's inner wall oriented at a 45° angle. Structures were always placed in the swim chamber prior to introducing fish into the respirometer. The cylinders represented simplified versions of common flow restoration structures, such as lunkers and root wads. The vertical support posts of a lunker are

Fig. 1. Photo of a 30 L swimming respirometer (*a*) utilized for accelerometer-tagged smallmouth bass swim trials and flow measurements, depicting the side (*b*) and top (*c*) views of the respirometer with relevant dimensions. The location of each tested structure, including the vertical structure (VS, *d*), the horizontal structure (HS, *e*), and the diagonal structure (DS, *f*) are depicted during vertical *XZ* plane tests. [Colour online.]
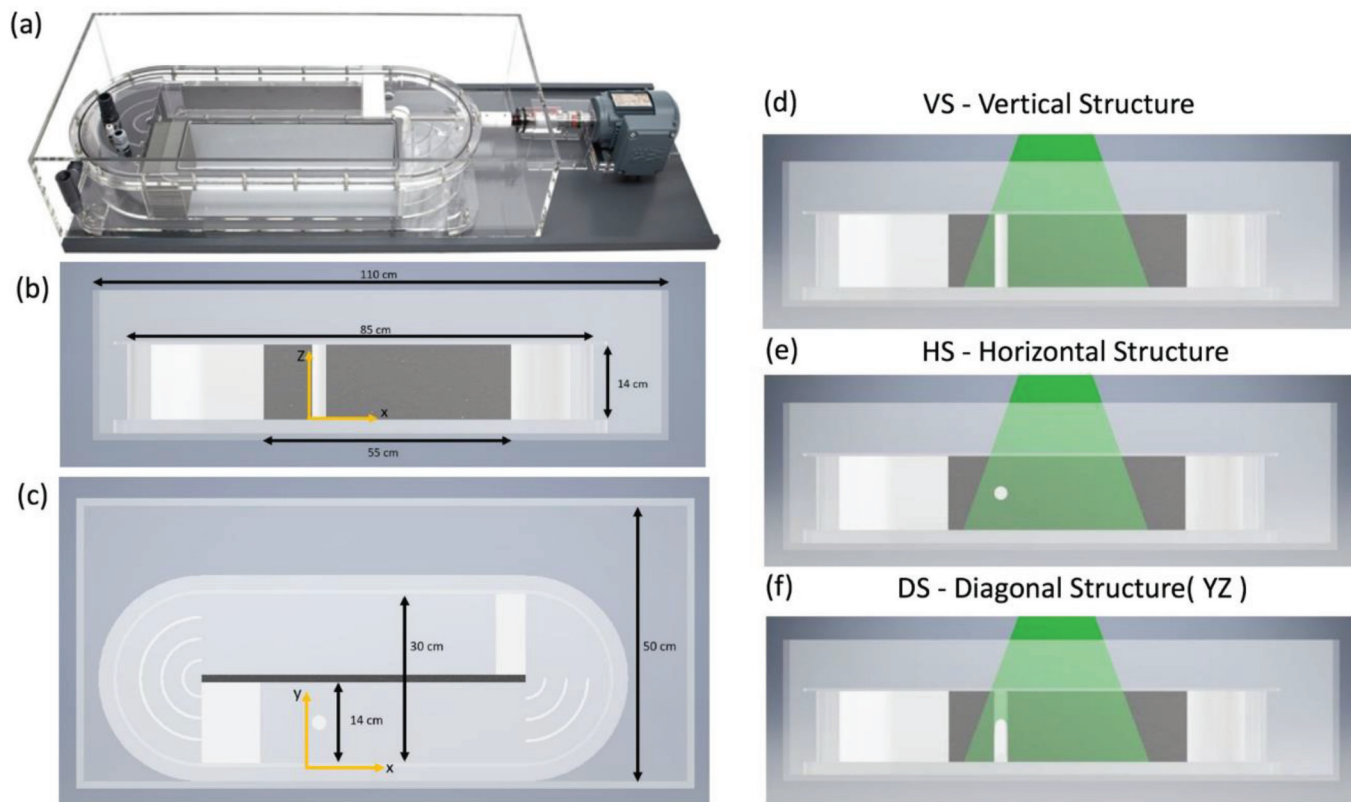
emulated by the vertical cylinder (Thompson 2005; Rosi-Marshall et al. 2006), whereas the complex structure of a root wad extending horizontally and diagonally into flow are represented by the horizontal and diagonal cylinders (Figs. 1*b*–1*f*) (Shirvell 1990; Manners and Doyle 2008).

Swimming trials were conducted between 3 and 21 December 2018. Tagged smallmouth bass, hereinafter referred to by structure treatment (HS, VS, DS, or NS) were randomly assigned to one of the four treatments. Each fish was only assigned to a single treatment in the study, and fish size did not differ across treatments (one-way analysis of variance (ANOVA) on body length (BL), $F_{[1,40]} = 1.4$, $P = 0.3$). The order that the study progressed was randomized in a three-tiered fashion intended to minimize the potential of temporal bias. First, tagged fish used in a trial were randomly chosen from the pool of all tagged individuals available on a given day. Second, for days in which fish from multiple acclimation temperatures were scheduled to swim, the order in which temperature treatments occurred was randomized, and the water within the respirometer was drained and refilled as needed. Finally, the order that structures were added to the swimming respirometer at a given temperature was also randomized. Following introduction into the swimming respirometer, smallmouth bass were acclimated at 0.5 BL·s⁻¹ for 30 min until normal behavior resumed (Peake et al. 1997; Cooke et al. 2001), indicated by the fish facing upstream and maintaining position within the swim chamber (Kern et al. 2018).

Following the acclimation period, water velocity in the respirometer was increased to 1.0, 1.5, 2.0, 2.5, and 3.0 BL·s⁻¹ (where 1.0 BL·s⁻¹ approximates 0.30 m·s⁻¹); approximate water velocity

was determined via a pre-existing conversion relating tunnel motor revolutions per minute (rpm) to water velocity (m·s⁻¹), initially generated with a flow meter (HFA, Höntzsch GmbH, Waiblingen, Germany). Water velocities were chosen based on previous measurements of critical swimming speed in similarly sized smallmouth bass (Peake 2004). One measurement of MO_2 was obtained at each of the six water velocities (Bouyoucos et al. 2017). During the swimming trial, the program AutoResp version 1 (Loligo Systems, Viborg, Denmark) was used to quantify MO_2. For all trials, the length of the mix phase of each measurement cycle was held constant at 1 min; the length of each flush phase was set at 3 or 4 min, depending on the flush pump in use. To obtain a high coefficient of determination (r^2 value) across different flow velocities, we varied the time of the measurement period (closed phase) from 4 to 15 min. Only MO_2 values with an r^2 value above 0.9 were included in this study (Svendsen et al. 2016). Trials ended either when a fish had successfully completed swimming at all five velocities, if a fish fell to the grate at the rear of the swimming chamber and refused to swim, or if a measurement period exceeded 15 min, a commonly used measurement period in similar studies (Bouyoucos et al. 2017; Brownscombe et al. 2018). Upon completion, each fish was removed from the respirometer and euthanized via an overdose of tricaine methanesulfonate (MS-222). The entire respirometer was cleaned with a bleach solution prior to trials beginning and regularly until all trials were completed. MO_2 measurements of the empty respirometer were obtained regularly to assess any background microbial respiration, which was found to be negligible (Rodgers et al. 2016).

Flow measurements

PIV was used to measure the velocity field within the respirometer on two two-dimensional (2D) planes within the test section: (*i*) a vertical plane oriented along the direction of the flow (*XZ* plane) at the tank centerline and (*ii*) a horizontal plane oriented along the direction of the flow (*XY* plane) at mid-depth. According to our reference frame, we define the components of the velocity as *u* in the longitudinal direction (*X*), *v* in the transverse direction (*Y*), and *w* in the vertical direction (*Z*). We use lowercase symbols (*u*, *v*, *w*) to indicate instantaneous values and uppercase for time averages (*U*, *V*, *W*; Fig. 1). A 5 W, 532 nm, continuous-wave laser (PIV-01251 DPSS, OptoEngine LLC, Midvale, Utah) coupled with a 45° cylindrical lens was used to generate a vertical or horizontal light-sheet (with a thickness < 1 mm) for illuminating particles traveling within the illuminated plane (11–18 μm diameter spherical glass particles; Fig. 1*d*–1*f*). A monochromatic camera (JAI GO-5000M-USB; JAI Inc., San Jose, California) captured 12-bit images with a 2560 × 2048 pixel resolution at frequencies from 30 to 60 frames per second. Trials with the investigated scenarios, NS, VS, HS, and DS, were run at respirometer motor frequencies of 108, 161, and 200 Hz, equivalent to mean longitudinal velocities of $U1 = 0.09$, $U2 = 0.18$, and $U3 = 0.24$ m·s^{-1}, respectively.

Jerk acceleration data processing and statistical analysis

The accelerometer tags used in this study yielded data in the form of jerk acceleration (i.e., change in acceleration between two successive times of measurement), summed in all three axes of movement (*X*, *Y*, and *Z*). For a given data point at time t_x, a jerk acceleration value greater than zero corresponds to a change in acceleration relative to acceleration at time t_{x-1} (i.e., a "jerk" or change in swimming acceleration); a jerk acceleration value equal to zero at t_x indicates an unchanged acceleration relative to acceleration at time t_{x-1}. Thus, when quantified over longer sampling intervals, periods of zero jerk acceleration indicate a consistent, smooth swimming gait, while nonzero values of jerk acceleration indicate that fish are changing gait and not swimming in a consistent fashion. Because the quantity of jerk acceleration data generated varied across fish and across trials (i.e., different oxygen measurement durations occurred at different water velocities), the total number of data points greater than zero and the number of data points equaling zero (referred to here as jerk and zero measurements, respectively) were first counted for each individual fish at a given swimming velocity. These counts were then used to create a response variable that consisted of the proportion of jerk accelerations relative to jerk acceleration values of zero for a fish at that swim velocity, as shown below:

$$\text{Jerk proportion} = \frac{\text{number of nonzero jerk measurements}}{\text{Total measurements}}$$

With this proportion as the response variable, data were modeled with a generalized linear mixed model that included structure treatment, water velocity, and temperature as fixed effects, structure treatment and water velocity as an interactive effect, and fish ID as a random effect (Bolker et al. 2009); structure and water velocity were interacted in all models due to this study's emphasis on the role of environmental conditions in affecting swimming stability and oxygen consumption. A linear mixed effects model was appropriate because multiple fixed effects, including water velocity, structure type, and temperature and their interactions were of interest and because the inclusion of individual fish across multiple swimming velocities involved repeated measures (Zuur et al. 2009). A beta-binomial distribution was used in the model not only to account for the fact that

the jerk acceleration data are proportions (zero or nonzero; Crowder 1978; Bolker et al. 2009), but also because of overdispersion of the data as indicated by residual deviance greater than the residual degrees of freedom (Ennis and Bi 1998; Crawley 2013). Model selection was based on fixed effects that best fit the data with the best fit defined by the model with the lowest AIC value (refer to the online Supplementary material, Table S1[1]) (Zuur et al. 2009; Crawley 2013). Owing to the large number of zero values in the data, a number of candidate zero-inflation models were also tested (Zuur et al. 2009); ultimately, the best-fitting model specified no zero inflation (Supplementary Table S1[1]). While it ultimately was not included in the best-fitting model, fish length was tested as a possible fixed effect because the effect of turbulence is related to how an eddy's diameter corresponds to a fish's length, whereby a fish is more likely to be affected when its length is similar to the diameter of the eddy (Lacey et al. 2012). Model fit was assessed through examination of predicted and observed quantile residuals for the overall model (i.e., quantile–quantile plots and examination of distribution of residuals), as well as for the structure and water velocity predictors (Pereira 2019). Possible effects of outliers or influential data points were considered to ensure that these effects were not present and did not influence model fitting (Zuur et al. 2009). Estimated marginal means were used to make post hoc pairwise comparisons between fixed effects (West et al. 2007).

Oxygen consumption statistical analysis

Because fish mass does not scale linearly with metabolic costs (Clarke and Johnston 1999), raw MO$_2$ data were transformed from mg O$_2$·kg^{-1}·h^{-1} to mass-independent mg O$_2$·h^{-1}. As with the jerk acceleration data, a linear mixed effects model was used to define the impacts of various fixed effects on MO$_2$. Water velocity, structure type, and temperature, interactions among these variables, and fish mass were included as fixed effects in models, with MO$_2$ treated as the dependent variable. Fish ID was specified as a random effect to account for the repeated sampling of the same individual across multiple swimming velocities (Crawley 2013). Additional models including respirometer swim trial date and days between surgical tagging and trial date as random effects were also tested. Model selection was based on the model that best fit the data, where the best fit corresponded to the model with the lowest AIC score (Supplementary Table S2[1]) (Crawley 2013). Both MO$_2$ and fish mass (g) were scaled logarithmically because the relationship between MO$_2$ and mass is not linear (Clarke and Johnston 1999; Killen et al. 2012). Interestingly, although temperature was included in the best-fitting model for jerk acceleration, the variable was not included in the best-fitting model for MO$_2$ (Supplementary Table S2[1]); the fixed effect factors ultimately included in the best-fitting MO$_2$ model were water velocity, structure treatment, the interaction between these two variables, and logarithmically scaled fish mass. The model fit for MO$_2$ data was assessed through a visual assessment of fitted residual and quantile–quantile plots (Zuur et al. 2009). Outlier tests were used to ensure that model fitting was not affected by influential data points (Zuur et al. 2009). Estimated marginal means were used to make post hoc pairwise comparisons between fixed effects terms (West et al. 2007).

All data derived from swim trials were processed and analyzed in R (version 3.6.0, R Foundation for Statistical Computing, Vienna, Austria). The package "lme4" version 1.1-21 (Bates et al. 2015) was used to estimate mixed effects models for MO$_2$ data, while "glmmTMB" version 0.2.3 (Brooks et al. 2017) was used to analyze jerk acceleration proportion data. Packages used for model selection include "car" version 3.0-3 (Fox and Weisberg 2019), "sjstats" version 0.15.5 (Lüdecke 2019), "rsq" version 1.1 (Zhang 2018), and "DHARMa" version 0.2.4 (Hartig 2019); "car"

---

was utilized to generate outlier and influential data plots, while "sjstats" and "rsq" were used to generate marginal and conditional r^2 values for each model, and "dHARMA" was used to generate quantile residuals for the best-fitting jerk acceleration model. Post hoc pairwise comparisons were made with "emmeans" version 1.3.4 (Lenth 2019). Figures were generated and arranged with "ggplot2" version 3.1.1 (Wickham 2016) and "cowplot" version 0.9.4 (Wilke 2019). The level of significance (α) for all tests was set at 0.05, and all reported are shown as $\pm$SE where appropriate.

Analysis of velocity statistics

PIV images were analyzed using Matlab-based (MathWorks R2017a) open source software PIVlab (version 2.02; Thielicke and Stamhuis 2014). Data analysis through PIVlab yielded 2D fields of instantaneous velocities u and v for horizontal XY planes and u and z for vertical XZ planes, with a spatial resolution of 3.2 mm. Plots of 2D time-averaged velocities in the longitudinal (U), transverse (V), and vertical direction (W) were obtained from the full time series of velocity data at each measurement location for all tested cases. Three turbulence metrics with potential effects on fish swimming capabilities were calculated (Lacey et al. 2012): Reynolds stresses, turbulent kinetic energy (TKE), and vorticity. Reynolds decomposition was used to calculate instantaneous velocity fluctuations u', v', and w' as

$$u' = u - U$$

$$v' = v - V$$

$$w' = w - W$$

Turbulent kinetic energy, TKE, is calculated in XZ and XY planes, respectively, as follows:

$$\text{TKE}_{XZ} = \frac{1}{2}\left(2\overline{u'^2} + \overline{w'^2}\right)$$

$$\text{TKE}_{XY} = \frac{1}{2}\left(2\overline{u'^2} + \overline{v'^2}\right)$$

Instantaneous fluctuations are used to calculate time-averaged (indicated by overbars) Reynolds stresses, $\overline{u'v'}$ and $\overline{u'w'}$. Components of vorticity, ω_y and ω_z, were calculated as the curl of the velocity vector, $\vec{\omega} = \nabla \times \vec{v}$, where $\vec{v} = (u, v, w)$. Reynolds stresses, TKE, and vorticity are all measures of the strength of turbulence that may affect fish swimming capabilities (Lacey et al. 2012).

To ensure all cases were within the fully turbulent wake regime (Williamson 1996), the Reynolds number (Re) based on cylinder diameter (d) was calculated for each case, yielding values of Re = Ud/ν = {1200, 5200, 6800}, where ν is the kinematic viscosity of water. To estimate the spatial effect of the structures, we calculated the cylinder wake wavelength (λ), the characteristic eddy frequency (f_p), and associated length scale (L_T). λ was calculated based on the shedding frequency (f), Strouhal number (St), and the mean velocity (U) as $\lambda = U/f$. Shedding frequency was estimated through St = fd/U using the expected value of St = 0.21 for the range of Re investigated (e.g., Liao et al. 2003a). Characteristic eddy frequency was obtained by computing the frequency spectra at each PIV subwindow and identifying the frequency f_p of the largest peak on the spectrum. The associated eddy length scales were computed as $L_T = T_T U$, where $T_T = 1/f_p$.

For a consistent comparison across all treatments, TKE, vorticity, and Reynolds stresses were converted to nondimensional form based on the undisturbed velocity U_∞ obtained from the temporal and spatial average of the case with no structure at

Table 2. Summary of the model relating structure treatment (diagonal, horizontal, vertical, or control), swimming velocity (10.0, 10.5, 20.0, 20.5, and 30.0 BL·s^{-1}), water temperature (15, 18, or 21 °C), and their interaction to the proportion of jerk measurements generated at a swimming velocity for smallmouth bass in a swimming respirometer.

	Estimate	Standard error	z value	Pr($>|z|$)
(Intercept)	−5.73	0.86	−6.61	<0.001
Diagonal	0.48	1.10	0.44	0.66
Horizontal	0.59	1.06	0.55	0.57
Vertical	0.12	1.15	0.10	0.92
1.5 BL·s^{-1}	2.76	0.79	3.51	<0.001
2.0 BL·s^{-1}	5.13	0.75	6.84	<0.001
2.5 BL·s^{-1}	5.81	0.75	7.74	<0.001
3.0 BL·s^{-1}	6.21	0.76	8.22	<0.001
18 °C	−0.36	0.48	−0.75	0.43
21 °C	0.82	0.52	1.59	0.11
Diagonal × 1.5 BL·s^{-1}	−2.15	1.19	−1.81	0.07
Horizontal × 1.5 BL·s^{-1}	−2.76	1.16	−2.38	0.02
Vertical × 1.5 BL·s^{-1}	−2.84	1.28	−2.23	0.03
Diagonal × 2.0 BL·s^{-1}	−4.13	1.14	−3.63	<0.001
Horizontal × 2.0 BL·s^{-1}	−4.17	1.06	−3.95	<0.001
Vertical × 2.0 BL·s^{-1}	−4.44	1.16	−3.82	<0.001
Diagonal × 2.5 BL·s^{-1}	−3.52	1.08	−3.25	<0.01
Horizontal × 2.5 BL·s^{-1}	−2.83	1.01	−2.80	<0.01
Vertical × 2.5 BL·s^{-1}	−3.64	1.10	−3.32	<0.001
Diagonal × 3.0 BL·s^{-1}	−3.48	1.08	−3.23	0.00
Horizontal × 3.0 BL·s^{-1}	−3.06	1.01	−3.00	<0.01
Vertical × 3.0 BL·s^{-1}	−3.14	1.08	−2.90	<0.01

Note: Fish ID was specified as a random effect. Results from model selection are shown in the online Supplementary Table 1[1], and data are visualized in Fig. 1a.

each flow rate and the diameter of the obstruction (i.e., TKE/U_∞^2, $\overline{u'w'}/U_\infty^2$, and $\omega_y d/U_\infty$). Values of nondimensional turbulence metrics were extracted and plotted for the vertical (XZ) and horizontal (XY) planes.
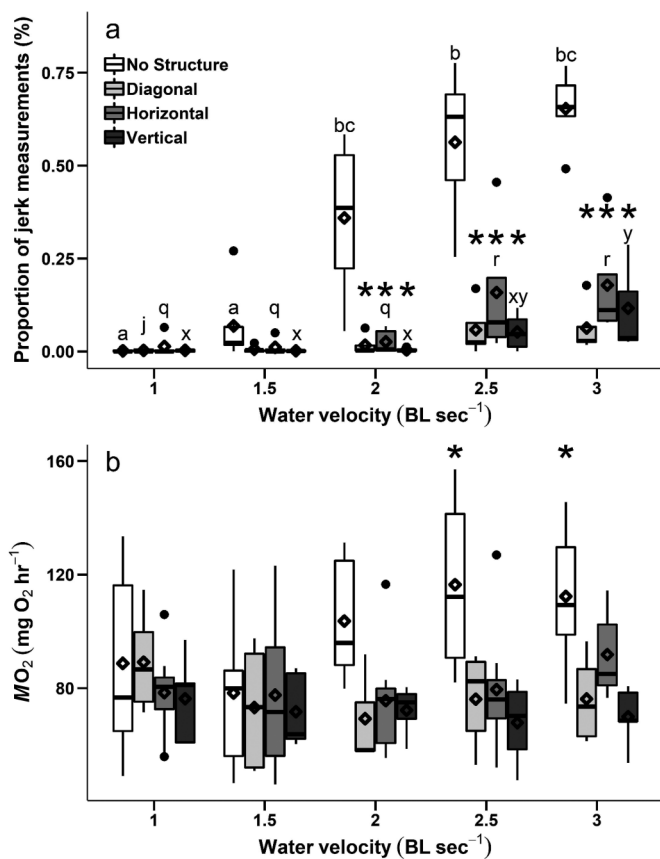
Results

Jerk acceleration

The model that best fit the jerk acceleration data, indicated by the lowest AIC score among the candidate models compared, included simulated structure, water velocity, and temperature as fixed effects, as well as the interactive effect of simulated structure and velocity. Although the inclusion of temperature improved the fit of the jerk acceleration model based on AIC score, it did not significantly impact proportion of jerk acceleration measurements (Table 2). All results are derived from post hoc pairwise comparisons.

Smallmouth bass swimming in the respirometer with no flow-modifying structures (NS treatment) did not differ significantly in proportion to jerk measurements when water velocity increased from 1.0 to 1.5 BL·s^{-1} (Table 2; Fig. 2a). As water velocity further increased beyond 1.5 BL·s^{-1} to 2.0, 2.5, and 3.0 BL·s^{-1}, the proportion of jerk acceleration movement in the NS treatment increased significantly with each increase in flow rate. At the highest flow rates of 2.5 and 3 BL·s^{-1}, the proportion of jerk acceleration measurements observed in the NS treatment was over 400 times greater than the proportion when fish were swimming at 1.0 BL·s^{-1}. In contrast, at 2.0, 2.5, and 3.0 BL·s^{-1}, the proportion of jerk measurements for fish swimming with any type of structure was significantly less than that for fish in the no structure treatment swimming at that same velocity (Fig. 2a; Table 2). The proportions of jerk measurements generated by smallmouth bass swimming in the respirometer with a diagonal structure (DS) at velocities greater than 1.0 BL·s^{-1} did not differ significantly from the proportion at 1.0 BL·s^{-1}, suggesting that the fish in this

Fig. 2. The proportion of jerk measurements (*a*) and oxygen consumption (in mg O$_2$·h^{-1}; *b*) by structure treatment and swimming velocity (BL·s^{-1}) for smallmouth bass acclimated to one of three different temperatures. For jerk acceleration, sample sizes varied from three to six fish per structure per swimming velocity. Letter assignments indicate a significant difference ($\alpha = 0.05$) across velocities within a given structure treatment: no structure (abc), diagonal, horizontal (qr), or vertical (xy). Asterisks (*) indicate a significant difference for a particular structure in comparison with the control treatment at that given swimming velocity. For oxygen consumption, sample size varied from two to nine fish per structure per swimming velocity, and asterisks indicate a significant difference between MO$_2$ at the given velocity and MO$_2$ for that same structure at 1.0 BL·s^{-1}. Diamonds represent the mean; circles represent outliers.

Table 3. Summary of model relating structure treatment (diagonal, horizontal, vertical, or control), swimming velocity (10.0, 10.5, 20.0, 20.5, and 30.0 BL·s^{-1}), fish mass, and the interaction of structure and swimming speed to oxygen consumption (MO$_2$) at a swimming velocity for smallmouth bass acclimated to one of three different water temperatures (15, 18, or 21 °C).

	Estimate	Standard error	df	*t* value	Pr(>|*t*|)
(Intercept)	−1.75	1.82	27.90	−0.96	0.34
Diagonal	0.17	0.15	52.89	1.15	0.25
Horizontal	−0.001	0.13	52.52	−0.05	0.96
Vertical	0.03	0.15	51.45	0.20	0.84
1.5 BL·s^{-1}	−0.05	0.08	96.25	−0.63	0.53
2.0 BL·s^{-1}	0.23	0.09	96.63	2.70	0.01
2.5 BL·s^{-1}	0.34	0.09	97.26	3.84	<0.001
3.0 BL·s^{-1}	0.36	0.09	97.29	4.04	<0.001
log(mass)	1.05	0.31	27.86	3.33	<0.01
Diagonal × 1.5 BL·s^{-1}	−0.16	0.14	96.64	−1.16	0.25
Horizontal × 1.5 BL·s^{-1}	0.02	0.12	96.43	0.15	0.88
Vertical × 1.5 BL·s^{-1}	−0.01	0.13	96.04	−0.08	0.94
Diagonal × 2.0 BL·s^{-1}	−0.47	0.14	96.56	−3.43	<0.001
Horizontal × 2.0 BL·s^{-1}	−0.28	0.12	96.29	−2.39	0.02
Vertical × 2.0 BL·s^{-1}	−0.34	0.14	96.49	−2.43	0.02
Diagonal × 2.5 BL·s^{-1}	−0.58	0.14	96.83	−4.14	<0.001
Horizontal × 2.5 BL·s^{-1}	−0.30	0.12	96.90	−2.46	0.01
Vertical × 2.5 BL·s^{-1}	−0.37	0.14	96.49	−2.74	0.01
Diagonal × 3.0 BL·s^{-1}	−0.65	0.14	97.04	−4.64	<0.001
Horizontal × 3.0 BL·s^{-1}	−0.18	0.12	96.82	−1.46	0.14
Vertical × 3.0 BL·s^{-1}	−0.43	0.14	96.50	−3.17	<0.01

Note: Both oxygen consumption and fish mass were log-transformed. Fish ID was specified as a random effect. Results from model selection are shown in the online Supplementary Table 2[1], and data are visualized in Fig. 1*b*.

best-fitting model (Supplementary Table S2[1]). The MO$_2$ of smallmouth bass swimming with structures did not differ across water velocities; even at the highest velocities of 2.5 and 3.0 BL·s^{-1}, MO$_2$ did not differ significantly from MO$_2$ at 1.0 BL·s^{-1} (Fig. 2*b*). In contrast, fish swimming without a structure experienced an increase in MO$_2$ of about 20%, relative to MO$_2$ at 1.0 BL·s^{-1}, at 2.5 and 3.0 BL·s^{-1} (Fig. 2*b*). However, at a given water velocity, MO$_2$ did not differ significantly for fish swimming with or without a structure (Table 3).

Flow characteristics

Water velocity was highest overall throughout the test section for tests without a simulated structure (Fig. 3). Alternating bands of high and low velocity along the *Y* axis highlighted the effect of the flow-redirecting vanes at the end of the tunnel (Fig. 4). Although this banding was evident to some extent in the tests with structures, it was clearly overwhelmed by the effect of the structures on the flow.

Pockets of reduced velocity developed in the lee of all structures, which produced a wake effect in the corresponding plane of orientation (Williamson 1996): the *XZ* (vertical) plane for the HS (Fig. 3) and the *XY* (horizontal) plane for the VS (Fig. 4). The DS produced a diagonal wake in both the *XZ* and *XY* planes (Figs. 3 and 4). A clear zone of recirculating fluid existed behind all structures (Figs. 3 and 4 — VS, HS, DS). Since only one diameter was tested, wake wavelength remained similar across all cases, at $\lambda \approx$ 0.12 m, with shedding frequencies *f* = [0.7, 1.5, and 2.0] Hz corresponding to bulk velocities *U* = [0.09, 0.18, 0.24] m·s^{-1}.

Patterns of TKE, vorticity, and Reynolds stresses (Figs. 5–9) clearly illustrated the influence of the simulated structures on turbulence. For the NS case, TKE, vorticity, and Reynolds stresses were relatively uniform in the *XZ* plane (Fig. 5), but the deflecting

treatment maintain a smooth swimming gait across all velocities (Table 2; Fig. 2*a*). In fact, the proportion of jerk measurements generated by smallmouth bass swimming with a DS at velocities of 2.0 and 2.5 BL·s^{-1} was significantly less than the proportions of NS fish swimming in the HS treatment showed a 12-fold increase in the proportion of jerk measurements at 2.5 and 3.0 BL·s^{-1} relative to proportions at 1.0 BL·s^{-1} (Table 2; Fig. 2*a*). Fish in the VS treatment also displayed significantly higher proportion of jerk measurements relative to 1.0 BL·s^{-1}, but only when swimming velocity increased to 3.0 BL·s^{-1} (Table 2; Fig. 2*a*). While differences between different structures at a given velocity were not significant, DS fish consistently had the lowest proportion of jerk measurements at high velocities, followed by VS fish and then HS fish.

Oxygen consumption

For MO$_2$ data, the best-fitting model included the interaction between simulated structure and velocity as well as the log of fish mass (g); temperature was not included as a parameter in the

Fig. 3. Time-averaged longitudinal velocity field (U; m·s^{-1}) on the vertical XZ plane tested within a 30 L swimming respirometer. Velocity fields are visualized for all four structure treatments (no structure (NS), vertical structure (VS), horizontal structure (HS), and diagonal structure (DS)) at each of the three velocities ($U1$, $U2$, $U3$) investigated. [Colour online.]
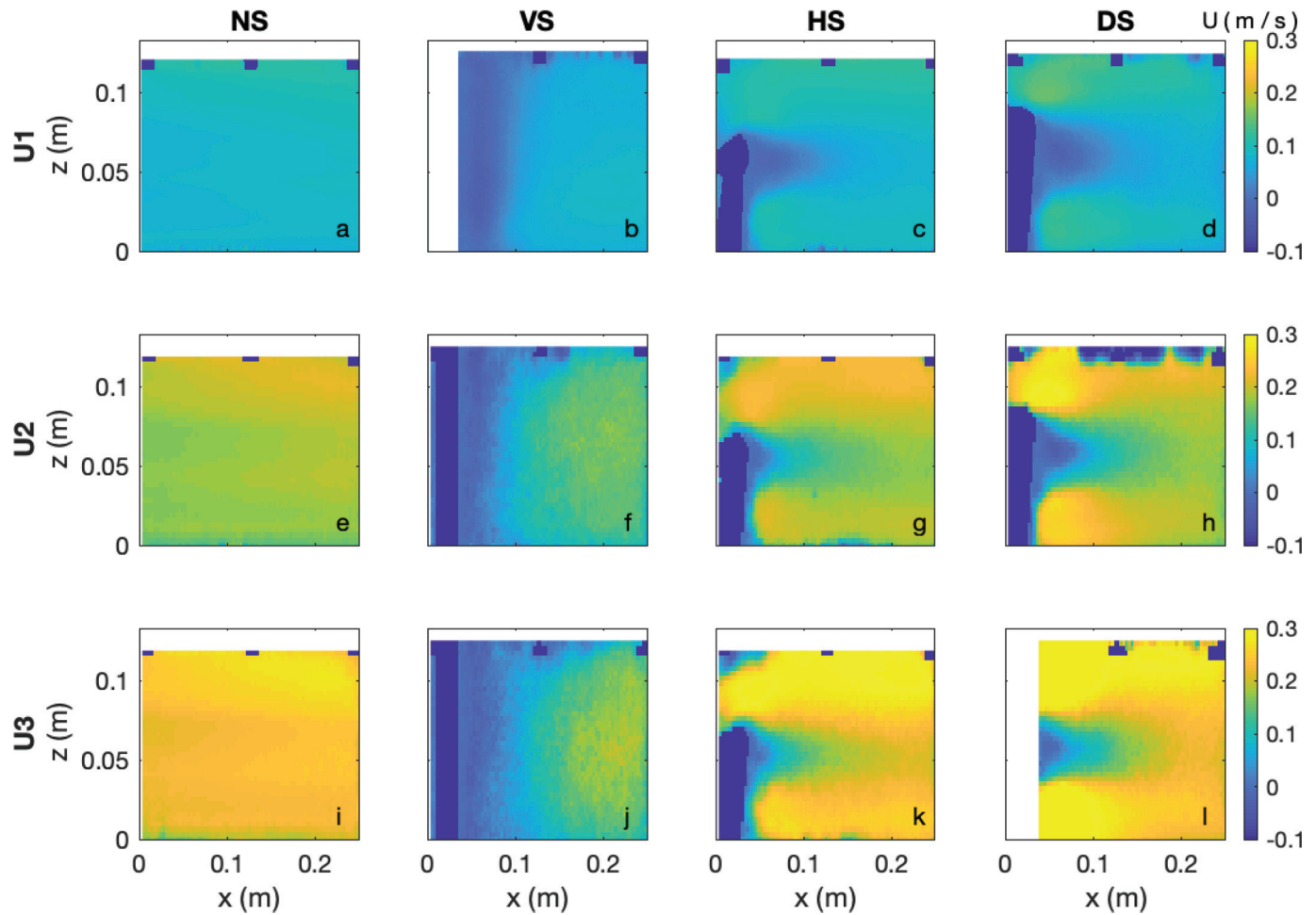
vanes had an effect on mean velocity and vorticity in the XY plane (Figs. 4 and 6). Nondimensional profiles of TKE, vorticity, and Reynolds stresses in the XZ (Fig. 7) and XY (Fig. 8) planes confirm that even in the horizontal plane, the flow was dominated by the cylindrical structures. The vanes had the biggest impact on the vertical component of vorticity (Fig. 8), but did not substantially affect TKE and Reynolds stress. Magnitudes of TKE and Reynolds stress for NS were an order of magnitude lower than those for the VS, HS, and DS (Figs. 7 and 8). A 2D analysis of eddy frequency (f_p) and eddy length scale (L_T) (Figs. 5j–5o and 6j–6o) shows that although the vorticity magnitude was of similar order for NS and VS, the vorticity for NS resulted from fast, small eddies produced by the inlet conditions that have length scales much smaller than fish size. Such eddies do not have substantial effects on fish.

High TKE values were present downstream of the structures, with a wake in the vertical plane formed in the lee of the HS (Fig. 5b), a wake in the horizontal plane generated behind the VS (Fig. 6b), and a diagonal wake formed behind the DS (Figs. 5c and 6c). Positive and negative patterns of vorticity (Figs. 5d–5f and 6d–6f) and Reynolds stress (Figs. 5g–5i and 6g–6i) on each side of the wake clearly show that opposing patterns of fluid rotation occurred in shear layers bounding the wakes and that vortex shedding produced a Karman vortex street downstream of the structures. The DS produced a noticeably wider spread of vortex

shedding compared with the VS and HS. Nondimensional transects of TKE, vorticity, and Reynolds stresses show that enhanced turbulent conditions were present for all structures for the full range of velocities investigated in this study (Figs. 7 and 8). The DS enhanced TKE, vorticity, and Reynolds stresses both in the horizontal and vertical planes, while the VS and HS enhanced these parameters only in the XY and XZ planes, respectively.

Discussion

The results of this study show that the presence of structures in the respirometer alters characteristics of the mean flow and turbulence, which in turn alters fish swimming behavior and fish energy expenditure.

Jerk acceleration

The presence of simulated structures in the respirometer resulted in a smoother swimming (i.e., less "jerky") gait for smallmouth bass. Fish swimming with structures experienced a significantly lower proportion of nonzero jerk measurements relative to fish in the control treatment, likely due to altered flow characteristics. Unobstructed flow is naturally turbulent, but does not develop coherent turbulent structures to the degree that flow does when physical structures are present (Robinson 1991). Immersed structures generate wakes, or zones of reduced

Fig. 4. Time-averaged longitudinal velocity field (U; m·s^{-1}) on the horizontal XY plane tested within a 30 L swimming respirometer. Velocity fields are visualized for all four structure treatments (no structure (NS), vertical structure (VS), horizontal structure (HS), and diagonal structure (DS)) at each of the three velocities ($U1$, $U2$, $U3$) investigated. [Colour online.]
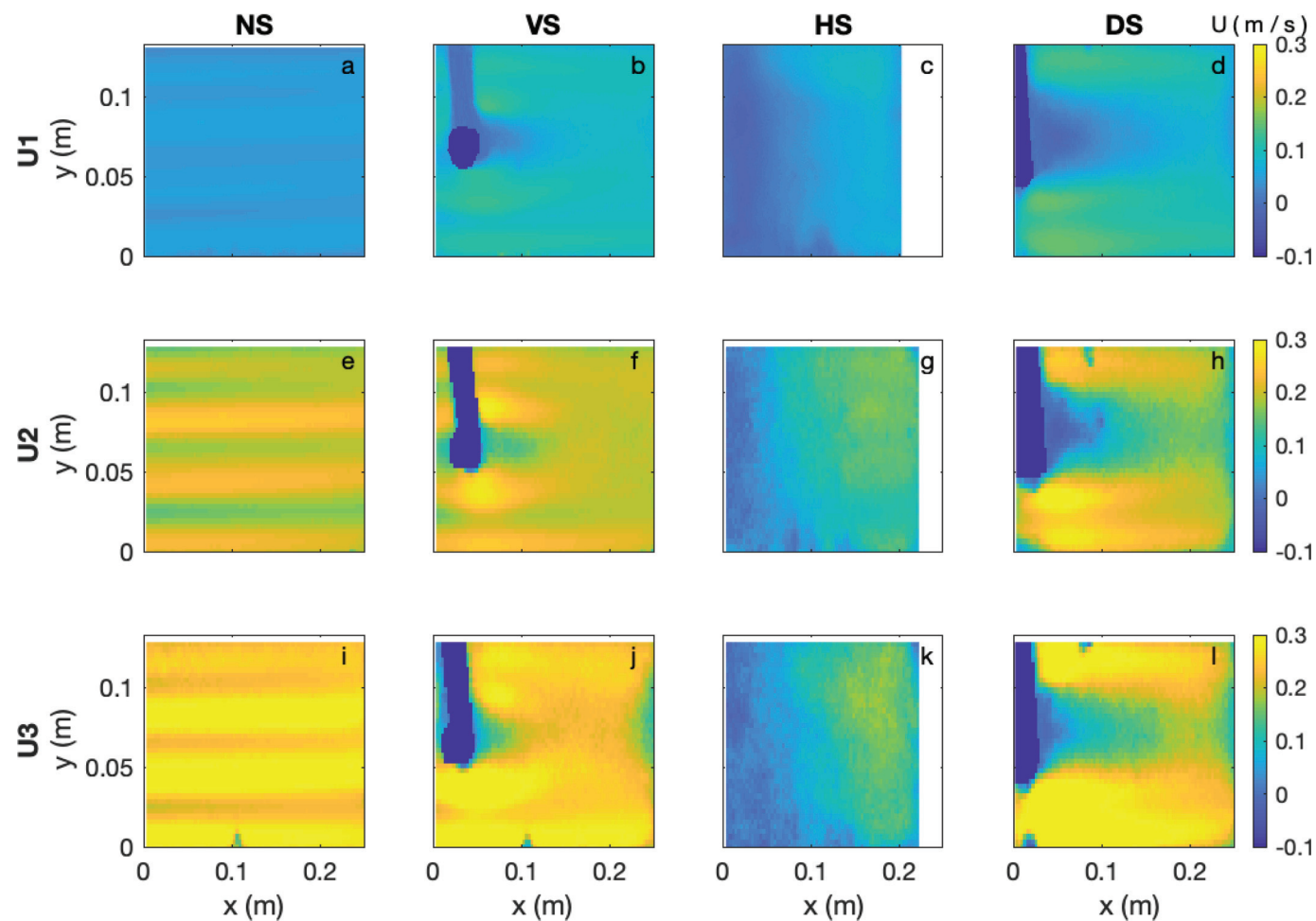

velocity, downstream of the structures, and both the shear layers bounding the wakes as well as vortices shed from the wakes produce high levels of vorticity and TKE (Williamson 1996). Generally, the results indicate that structures confer benefits when fish are interacting with turbulent flow immediately downstream of these structures by improving swimming stability, especially for flows with high mean velocities within the ranges used in this study (Figs. 5 and 6).

Smallmouth bass swimming with structures experienced a lower proportion of jerk acceleration measurements and were able to maintain a more stable swimming position (i.e., lower proportion of jerk measurements), particularly at swimming speeds above 2 BL·s^{-1}, likely due to their utilization of the flow conditions generated by the structures. These fish were likely able to exploit pockets of reduced velocity as refugia from the relatively high velocity in other areas of the flow (identified as low-velocity areas in Figs. 3 and 4, corresponding to high vorticity as shown in Figs. 5 and 6), thereby resulting in a smooth swimming gait and a reduced proportion of jerk measurements at a given swimming speed compared with NS fish. Alternatively, smallmouth bass may also have coordinated their swimming mechanics with characteristics of coherent turbulent structures generated by simulated structures. The ability of certain fish species to exploit turbulence has been well-documented (Liao 2007). Previous laboratory studies have

shown that rainbow trout (*Oncorhynchus mykiss*) reduce muscle activity when swimming in turbulent eddies shed by cylinders by utilizing a unique swimming gait known as the Kármán gait (Liao et al. 2003a; Liao 2004); this gait allows trout to essentially slalom between eddies and reduce their need for powered swimming. Others have shown that when fish swim in the turbulent flows generated within a school, they have lower tail-beat frequencies than fish swimming alone, likely due to interactions with vortices shed by other members of the school (Svendsen et al. 2003). Smallmouth bass may potentially be capable of exploiting turbulent vortices as well and may have utilized such a swimming strategy in this study.

While the zones of reduced velocity behind each structure can be beneficial regardless of orientation, the orientation of a vortex affects whether it can be exploited by fish. Flow analyses characterizing flow on vertical and horizontal planes for three structure orientations (HS, VS, and DS) demonstrated the similarities of generated wakes in their respective planes (Figs. 7 and 8), allowing for the assessment of a broad range of Re and TKE levels. Direct comparison across treatments (Fig. 9) displayed the various patterns generated by the three orientations, allowing for the identification of specific zones that may work as attractors or distractors for fish swimming behind such structures based not only on bulk velocity, but also on turbulence and vorticity

Fig. 5. Time-averaged turbulent kinetic energy field (TKE; m²·s⁻²) (*a–c*), vorticity (ω_y; s⁻¹) (*d–f*), Reynolds stresses ($\overline{u'w'}$; m²·s⁻²) (*g–i*), eddy frequency (f_p; Hz) (*j–l*), and eddy length scale (L_T; m) (*m–o*) on the *XZ* plane for no structure (NS), horizontal structure (HS), and diagonal structure (DS), respectively, at the highest velocity, *U3* (0.24 m·s⁻¹). [Colour online.]
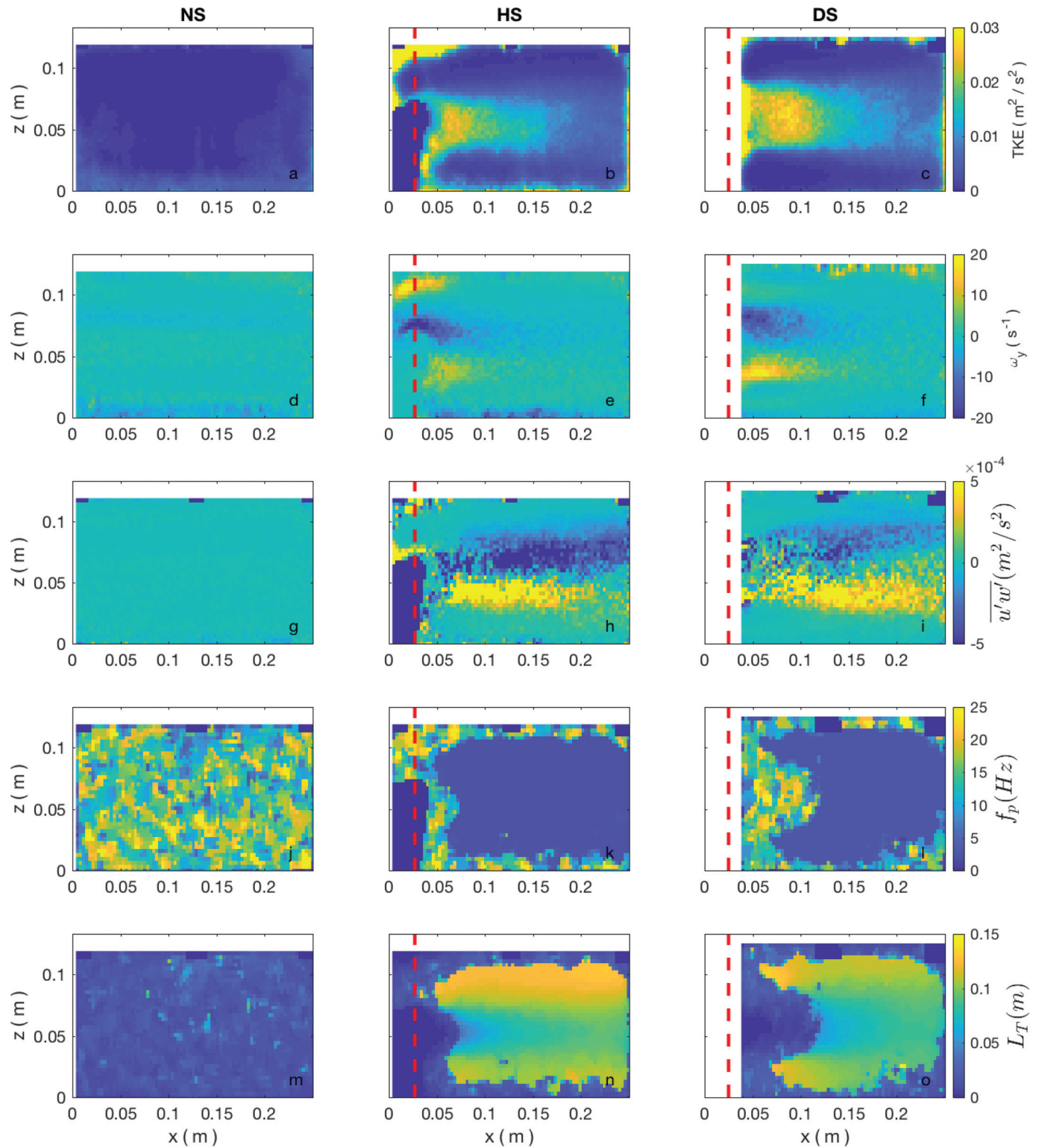
metrics. Typically, horizontally oriented vortices, such as those generated by the VS, can be exploited by fish (Liao et al. 2003*b*; Taguchi and Liao 2011), reducing their need for powered swimming, while vertically oriented vortices, such as those generated

by the HS, may destabilize fish (Tritico and Cotel 2010; Maia et al. 2015). These documented relations may explain why smallmouth bass in the DS treatment, which included both the development of a zone of low velocity behind the structure and horizontally

50

Can. J. Fish. Aquat. Sci. Vol. 78, 2021

Fig. 6. Time-averaged turbulent kinetic energy field (TKE; $m^2 \cdot s^{-2}$) (a–c), vorticity (ω_z; s^{-1}) (d–f), Reynolds stresses ($\overline{u'v'}$; $m^2 \cdot s^{-2}$) (g–i), eddy frequency (f_p; Hz) (j–l), and eddy length scale (L_T; m) (m–o) on the XY plane for no structure (NS), vertical structure (VS), and diagonal structure (DS), respectively, at the highest velocity, U3 (0.24 m·s^{-1}). [Colour online.]
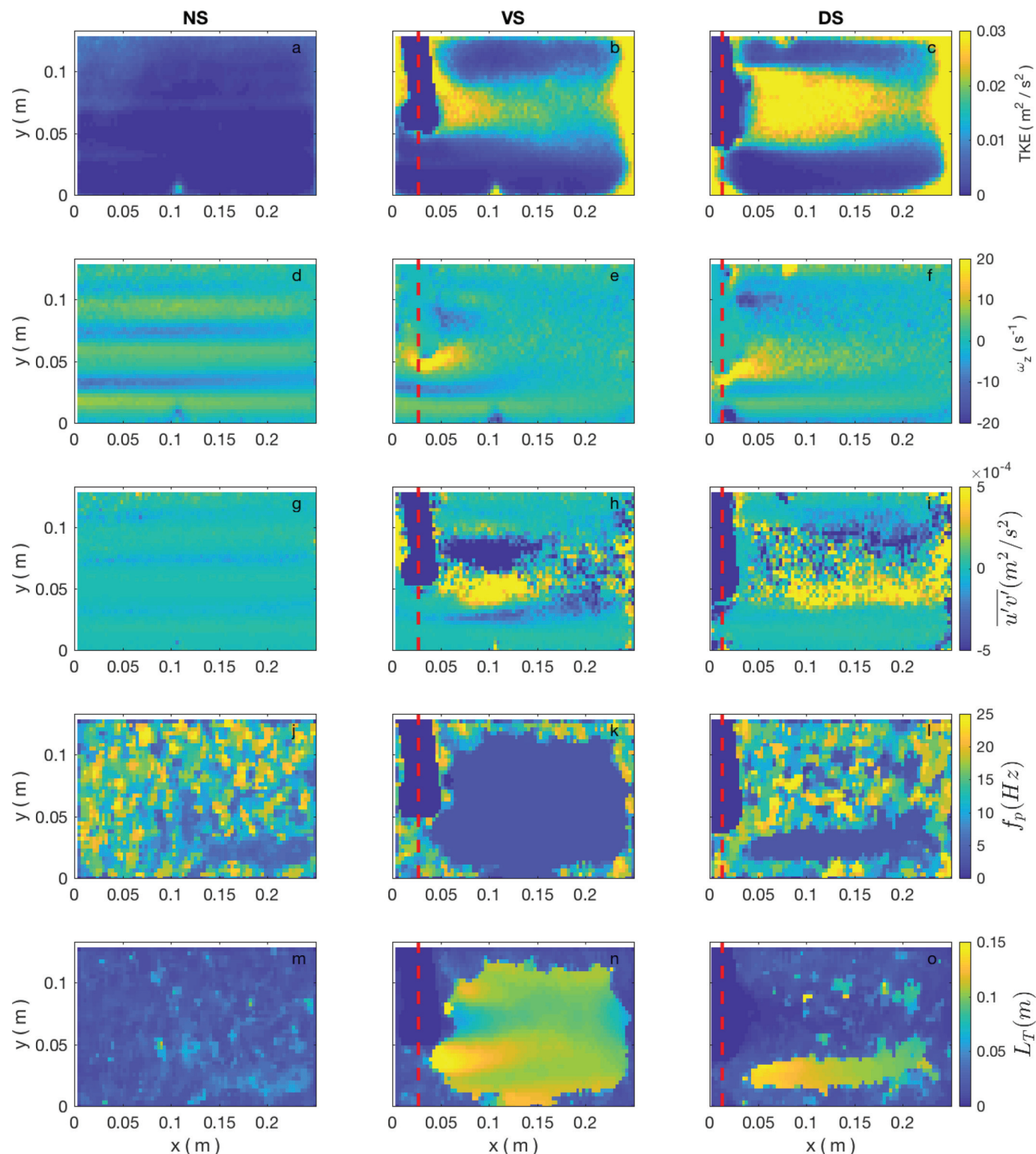

oriented vortices, experienced no increases in jerk acceleration across water velocities. On the other hand, HS fish, which were exposed to potentially destabilizing vertically oriented vortices, experienced a higher number of jerk accelerations at high velocities than either DS or VS fish.

Oxygen consumption

The presence of simulated structures provided an energetic advantage for smallmouth bass relative to fish in the control (NS treatment), particularly when water velocities reached 2.5 BL·s^{-1}. More specifically, the MO_2 of smallmouth bass swimming with

Fig. 7. Nondimensional temporally and spatially averaged (over the *x* direction) vertical profiles of turbulent kinetic energy (TKE; left column), vorticity (ω_y; middle column), and Reynolds stresses ($\overline{u'w'}$; right column), measured at the highest velocity (U3, 0.24 m·s^{-1}) on a vertical *XZ* plane, for the cases with no structure (NS), horizontal structure (HS), and diagonal structure (DS). Values are made nondimensional using the undisturbed velocity U_∞. [Colour online.]
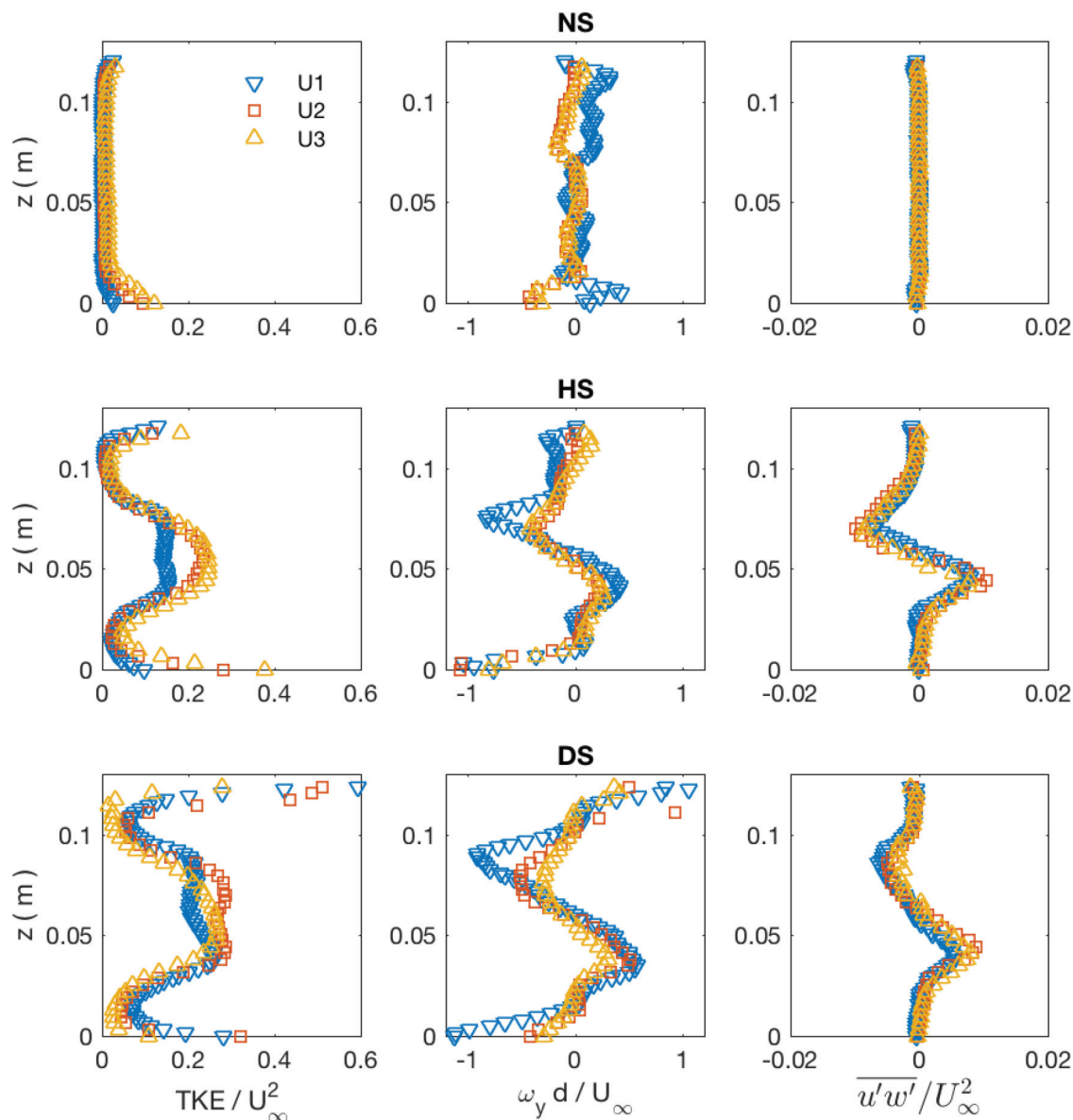
structures did not differ across water velocities, whereas smallmouth bass swimming with no structure in the respirometer had higher MO$_2$ at 2.5 and 3.0 BL·s^{-1} relative to MO$_2$ at the lowest velocity. Energetic demand correlates positively with swim velocity for fish due to the increased recruitment of aerobic red muscle fiber necessary to power swimming (Coughlin 2002), which, in turn, results in an increase in MO$_2$ across swim speeds until anaerobic (burst) swimming occurs (Beamish 1970; Webb 1971). Certain fish species have previously been shown to reduce MO$_2$ when swimming with structures or swimming in enhanced turbulent conditions (Liao 2007). Rainbow trout, for example, are able to employ specific swimming gaits, including the Kármán gait, and may preferentially position themselves in turbulent flow generated by cylinders to consume less oxygen when swimming (Cook and Coughlin 2010; Przybilla et al. 2010) and at times can decrease their MO$_2$ even when water velocity increases

(Taguchi and Liao 2011). Shiner perch (*Cymatogaster aggregata*) are also able to reduce MO$_2$ in turbulent flow, even when such flow is lacking in coherent vortical structures (van der Hoop et al. 2018). While no studies to date have demonstrated a similar gait in smallmouth bass, as a riverine species, this species may have some ability to exploit turbulent flow, similar to rainbow trout. Such behavior may account for the lack of an increase in MO$_2$ values, despite an increase in water velocity. Alternatively, smallmouth bass in the structure treatments may have simply positioned themselves in the low-velocity pockets behind each simulated structure (Fig. 9), thereby reducing swimming oxygen costs. Further work that examines in detail the swimming gait and position of fish in relation to structures is needed to determine which of these strategies was potentially at play. What the results do confirm is that smallmouth bass swimming in the presence of simulated structures maintained a consistent MO$_2$ across

Fig. 8. Nondimensional temporally and spatially averaged (over the *x* direction) transects of turbulent kinetic energy (TKE; left column), vorticity (ω_z; middle column), and Reynolds stresses ($\overline{u'v'}$; right column), measured at the highest velocity (*U*3, 0.24 m·s^{-1}) on a horizontal *XY* plane, for the cases with no structure (NS), horizontal structure (HS), and diagonal structure (DS). Values are made nondimensional using the undisturbed velocity U_∞. [Colour online.]
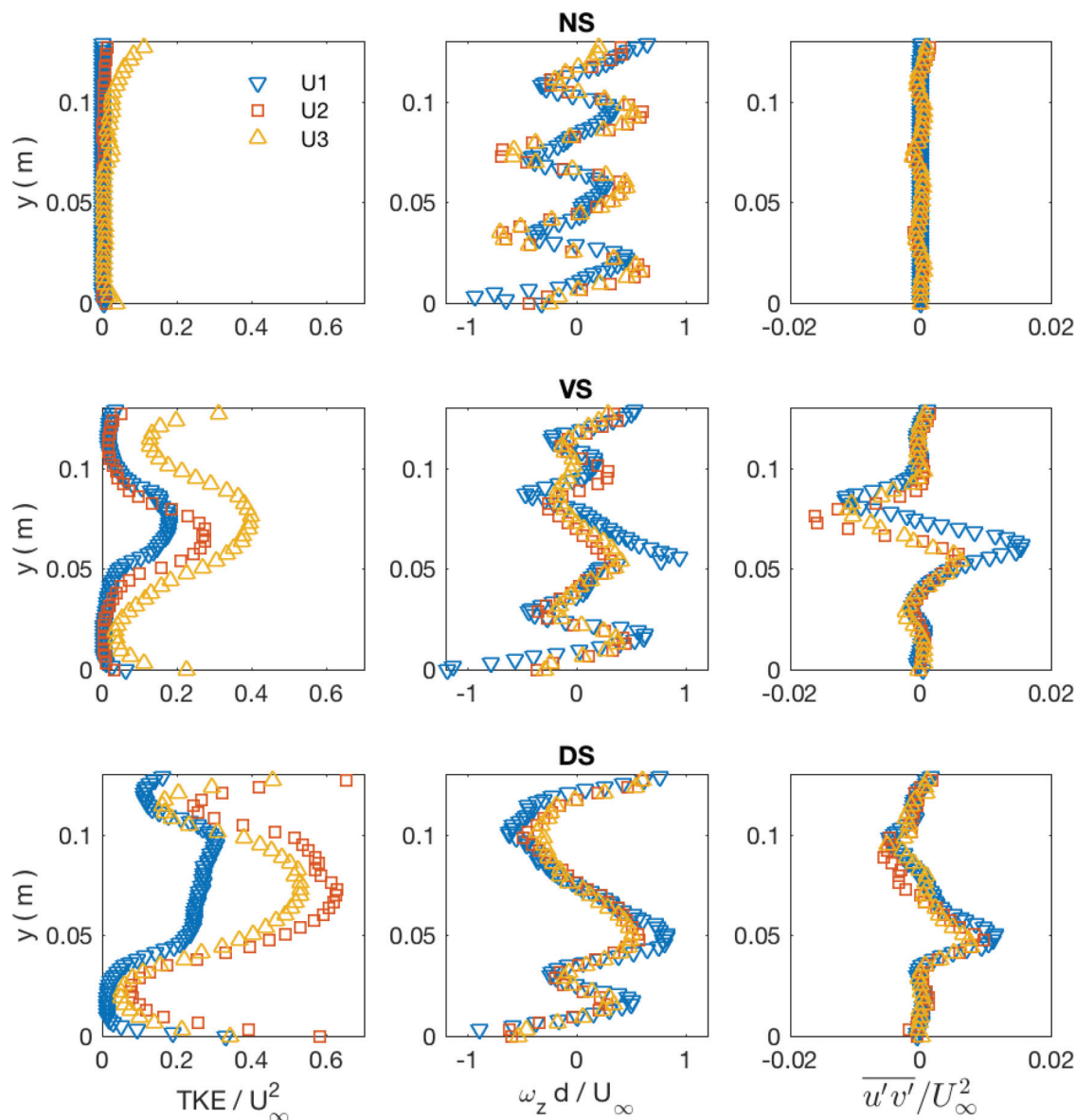
water velocities compared with fish swimming without simulated structures, which experienced pronounced increases in MO$_2$ at high velocities.

Interestingly, temperature was not a significant predictor in the best-fitting model for MO$_2$, indicating that the oxygen consumed by smallmouth bass in the swimming respirometer did not vary with temperature. MO$_2$ in fish normally correlates positively with temperature, with fish consuming greater amounts of oxygen at higher temperatures (Enders and Boisclair 2016). Three explanations are possible as to why temperature did not significantly relate to MO$_2$ in the current study. First, the range of temperatures may not have been sufficiently broad to result in a significant temperature relationship for smallmouth bass, which have a wide thermal range and high thermal tolerance. These fish commonly occur in environments where water temperatures may drop to near 0 °C in the winter and rise to well over 20 °C in the summer (Eaton

and Scheller 1996; Suski and Ridgway 2009). As such, varying temperature by 6 °C, from 15 to 21 °C, may not have been sufficient to produce differences in MO$_2$ over this range for such a eurythermal fish, which has evolved to tolerate a wide range of temperatures. Second, the temperatures used in the current study may not have been sufficiently distinct to generate significant differences in statistical models. Notably, when the impact of temperature on MO$_2$ was plotted across structure types (Supplementary Fig. S1[1]), the 15 and 21 °C treatments appeared to differ, whereas the 18 °C treatment had a wide range of MO$_2$ values across all structure types. Indeed, if a simple ANOVA is performed with temperature included as the sole fixed effect and MO$_2$ as the response variable, MO$_2$ differs for fish swimming at 15 and 21 °C, but fish swimming at 18 °C do not differ significantly from the other two temperature treatments (Supplementary Table S3[1]). This analysis suggests that temperature may have an effect on MO$_2$, with higher amounts of oxygen consumed at the

Fig. 9. Temporally and spatially averaged (over the x direction) nondimensional profiles of velocity (U and W), vorticity (ω), turbulent kinetic energy (TKE), and Reynolds stresses ($\overline{u'v'}$) for all simulated structure cases (no structure (NS), vertical structure (VS), horizontal structure (HS), diagonal structure (DS)) at the fastest flow ($U3$, 0.24 m·s^{-1}). [Colour online.]
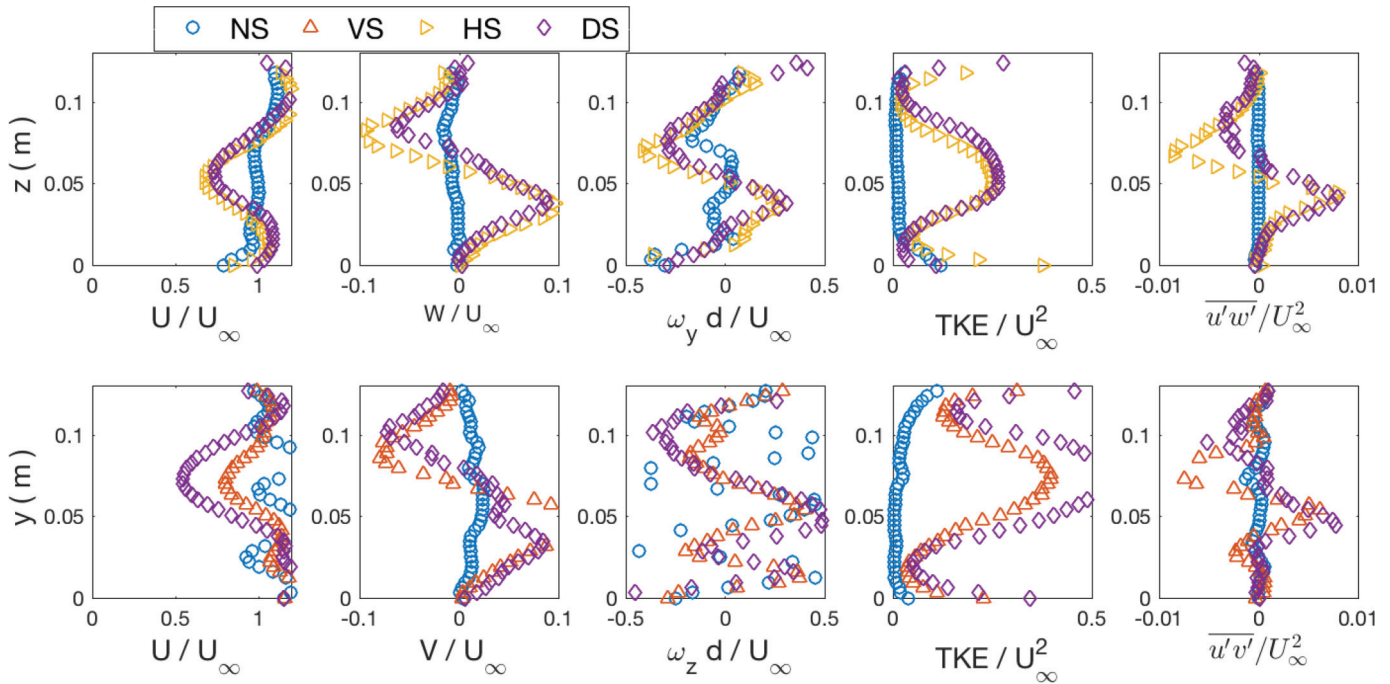
warmest treatment relative to the other treatments, but that the temperature effect was masked by strong effects from other factors. Lastly, the lack of a relation between temperature and MO$_2$ may be the result of reduced statistical power due to relatively small sample sizes and complex modeling procedures. To better account for thermal impacts on both swimming ability and MO$_2$, future studies should utilize a wider range of acclimation temperatures that more thoroughly represent the conditions commonly experienced by the study species in the wild.

Results from this study have three main implications for the use and design of instream restoration structures in relation to their physiological influence on stream-dwelling smallmouth bass. First, regardless of the orientation of a structure, its components, or the water temperature, restoration structures can confer energetic benefits for smallmouth bass when they are interacting with structures at short range. Thus, if a restoration project is being implemented and with the hope of providing shelter, cover, or energetic refugia for smallmouth bass, the inclusion of structures in the project may confer energetic benefits, especially at high water velocities. The addition of simulated structures, regardless of their orientation, produced pockets of reduced velocities and coherent turbulent structures that provide energetic advantages for fish. Second, energetic expenses (such as MO$_2$ rates) serve as an important physiologic metric for documenting short-term responses of fish to altered flow generated by instream structures. As such, energy expense may be a useful tool to supplement existing in situ monitoring for evaluating and monitoring the effectiveness of restoration projects. Such a tool can complement measures of population- and community-level changes following restoration, some of which may change only slowly over several years (Jeffrey et al. 2015). By providing insight into fish interactions with turbulent flow, an aspect of the environment known to strongly influence swimming performance, energetics may contribute, in conjunction with other metrics, to a more holistic understanding of population-level responses to instream structures and stream

restoration. Finally, at low velocities, structures conferred no apparent benefit for either energetic expense or position stability, but at high velocities, the value of structures became more pronounced, suggesting that the benefits of instream structures change across hydraulic contexts. While this potential threshold effect requires future study to relate precisely to fish response, these results suggest that the energetic benefits of structures may be most pronounced in fast-flowing rivers or during high-flow events when fully turbulent coherent flow structures are developed. On the other hand, structures may not provide energetic advantages in streams with consistently low flow velocities.

Caveats and future directions

Not all aspects of the relation between swimming energetics and flow characteristics could be explored in this laboratory investigation using a respirometer. Several caveats are identified that should be addressed in future work. First, although nondimensional turbulence statistics allow extrapolation of results of measured cases to those of unmeasured cases within the range of Re investigated (as shown in Figs. 7 and 8), turbulence statistics did not directly correspond to all mean flow velocities tested in swimming trials, limiting direct quantification of fish-flow interactions in this study. Second, conclusions from this study may be somewhat limited due to the physical constraints of the swimming respirometer, and results apply to smallmouth bass swimming immediately downstream from instream structures. Swimming respirometers have a defined swimming chamber to keep fish in a consistent location, and the size of the chamber and volume of water in the tunnel dictate the size of the fish that can be used. If fish are too small, MO$_2$ data are unreliable, and, in contrast, fish that are too large cannot move freely (Svendsen et al. 2016). In the current study, the fish were adequately sized for the tunnel and for the size of the accelerometer tags (Brown et al. 2004; Cooke et al. 2011), but were somewhat restricted in motion with little "choice" in which portion of the swim chamber they could occupy, in part due to the presence of structures.

As such, some uncertainty exists as to whether smallmouth bass were purposefully utilizing low-velocity pockets behind simulated structures and (or) coherent turbulent vortices generated by these structures. A critical need exists to utilize large flumes or field deployments in future work that allow fish unrestricted choice in position and enable tracking of fish positions, which in turn will allow for the precise evaluation of potential swimming strategies at play. Through such studies instantaneous swimming responses can be linked to local characteristics of the flow to provide improved insight into how much fish benefit from turbulent structures, low-velocity zones, or both. Large test environments will additionally allow for the investigation of interactions between fish and structure-generated turbulence as distance from the structure increases. Third, only a single structure diameter was investigated due to the size of the respirometer test section, limiting the size of eddies that could be generated. The influence of an eddy on a fish's swimming behavior depends in part on elements of scale, with eddies much smaller or larger than a fish having little effect on swimming, but eddies of diameters near the length of a fish being more likely to alter swimming kinematics and behavior (Lacey et al. 2012). Depending on the species, this may result in improved or reduced swimming performance (Lacey et al. 2012). Future studies with multiple combinations of BL:structure diameter ratio will allow detailed characterization of eddy size and eddy orientation. Despite these caveats, this study shows that structures do provide benefits to smallmouth bass both in terms of energetic expenses and position stability, particularly when smallmouth bass are swimming immediately downstream from the structures.

Conclusion

Although instream structures are a common tool for restoration of fish habitat in freshwater systems, the independent effects of these structures on fish energetics are poorly understood. This study utilized a laboratory approach to isolate how altered flows generated by simple simulated instream structures impact the energetic expense and swimming stability of smallmouth bass when they are swimming immediately behind the structures. Results showed that smallmouth bass swimming with structures were able to utilize altered flow conditions both to maintain a stable swimming position and to reduce energy expenditure compared with unaltered flow conditions in the absence of simulated structures. Interestingly, benefits of structures were most evident at high mean water velocities but were not statistically significant at low velocities. These findings provide direction for future laboratory or mesocosm studies investigating the interactions between smallmouth bass and restoration structures and additionally inform management aimed at the design, implementation, and augmentation of natural and artificial instream restoration structures by illustrating the hydraulic conditions in which instream structures may be most energetically beneficial for smallmouth bass. However, further work is needed to identify precisely the threshold velocities in natural streams that lead to energetic benefits by structures. Future investigations should move into larger laboratory spaces or beyond the lab, into the field, to directly estimate the energetic consequences of natural turbulent flows for fish, which is now possible due to recent advances in telemetry methods (Metcalfe et al. 2016) that allow indirect measurement of energetic expenses of free-swimming fish. The findings of this study may additionally illuminate particular flow conditions of interest in future field-based investigations. Subsequent studies as well as restoration monitoring efforts should continue to include physiological metrics to improve fish management and conservation (Young et al. 2006); while many factors impact the interactions between fish and instream structures, and the responses of fish communities to such restoration are complex, energetics, in particular, can clearly demonstrate the direct physiological responses of individual fish to altered flow conditions. By combining estimates of MO_2 with direct measurements of the flow field in spaces much larger than the typical respirometer, the effect of instream

structures of increased size and complexity, as well as arrangements of multiple structures, on fish energetics can be tested. Developing a more complete understanding of the role of energetics within the context of the many other ecological aspects of structures is a complex endeavor that will require multifactor field and experimental investigations in the future.

Acknowledgments

References

Abbe, T., and Brooks, A. 2011. Geomorphic, engineering, and ecological considerations when using wood in river restoration. *In* Geophysical monograph series. pp. 419–451.

Adams, N.S., Rondorf, D.W., Evans, S.D., Kelly, J.E., and Perry, R.W. 1998. Effects of surgically and gastrically implanted radio transmitters on growth and feeding behavior of juvenile Chinook Salmon. Can. J. Fish. Aquat. Sci. **127**(1): 128–136. doi:10.1577/1548-8659(1998)127<0128:EOSAGI>2.0.CO;2.

Angermeier, P.L., and Karr, J.R. 1984. Relationships between woody debris and fish habitat in a small warmwater stream. Trans. Am. Fish. Soc. **113**(6): 716–726. doi:10.1577/1548-8659(1984)113<716:RBWDAF>2.0.CO;2.

Antón, A., Elosegi, A., García-Arberas, L., Díez, J., and Rallo, A. 2011. Restoration of dead wood in Basque stream channels: effects on brown trout population. Ecol. Freshw. Fish. **20**(3): 461–471. doi:10.1111/j.1600-0633.2010.00482.x.

Bates, D., Mächler, M., Bolker, B.M., and Walker, S. 2015. Fitting linear mixed-effects models using lme4. J. Stat. Softw. **67**(1): 1–48. doi:10.18637/jss.v067.i01.

Beal, D.N., Hover, F.S., Triantafyllou, M.S., Liao, J.C., and Lauder, G.V. 2006. Passive propulsion in vortex wakes. J. Fluid Mech. **549**(1): 385–402. doi:10.1017/S0022112005007925.

Beamish, F.W.H. 1970. Oxygen consumption of largemouth bass, *Micropterus salmoides*, in relation to swimming speed and temperature. Can. J. Zool. **48**(6): 1221–1228. doi:10.1139/z70-211. PMID:5503024.

Beechie, T.J., Sear, D.A., Olden, J.D., Pess, G.R., Buffington, J.M., Moir, H., et al. 2010. Process-based principles for restoring river ecosystems. Bioscience, **60**(3): 209–222. doi:10.1525/bio.2010.60.3.7.

Bennett, S.J., Ghaneeizad, S.M., Gallisdorfer, M.S., Cai, D., Atkinson, J.F., Simon, A., and Langendoen, E.J. 2015. Flow, turbulence, and drag associated with engineered log jams in a fixed-bed experimental channel. Geomorphology, **248**: 172–184. doi:10.1016/j.geomorph.2015.07.046.

Bernhardt, E.S., and Palmer, M.A. 2007. Restoring streams in an urbanizing world. Freshw. Biol. **52**(4): 738–751. doi:10.1111/j.1365-2427.2006.01718.x.

Bernhardt, E.S., Palmer, M.A., Allan, J.D., Alexander, G., Barnas, K., Brooks, S., et al. 2005. Synthesizing U.S. river restoration efforts. Science (80-.), **308**(5722): 636–637. doi:10.1126/science.1109769.

Bernhardt, E.S., Sudduth, E.B., Palmer, M.A., Allan, J.D., Meyer, J.L., Alexander, G.G., et al. 2007. Restoring rivers one reach at a time: results from a survey of U.S. river restoration practitioners. Restor. Ecol. **15**(3): 482–493. doi:10.1111/j.1526-100X.2007.00244.x.

Boavida, I., Santos, J.M., Cortes, R.V., Pinheiro, A.N., and Ferreira, M.T. 2011. Assessment of instream structures for habitat improvement for two critically endangered fish species. Aquat. Ecol. **45**(1): 113–124. doi:10.1007/s10452-010-9340-x.

Bolker, B.M., Brooks, M.E., Clark, C.J., Geange, S.W., Poulsen, J.R., Stevens, M.H.H., and White, J.-S.S. 2009. Generalized linear mixed models: a practical guide for ecology and evolution. Trends Ecol. Evol. **24**(3): 127–135. doi:10.1016/j.tree.2008.10.008. PMID:19185386.

Bouyoucos, I.A., Montgomery, D.W., Brownscombe, J.W., Cooke, S.J., Suski, C.D., Mandelman, J.W., and Brooks, E.J. 2017. Swimming speeds and metabolic rates of semi-captive juvenile lemon sharks (*Negaprion brevirostris*, Poey) estimated with acceleration biologgers. J. Exp. Mar. Biol. Ecol. **486**: 245–254. doi:10.1016/j.jembe.2016.10.019.

Brooks, M.E., Kristensen, K., van Benthem, K.J., Magnusson, A., Berg, C.W., Nielsen, A., et al. 2017. glmmTMB balances speed and flexibility among packages for zero-inflated generalized linear mixed modeling. R Journal, **9**(2): 378–400. Available from https://journal.r-project.org/archive/2017/RJ-2017-066/index.html. doi:10.32614/RJ-2017-066.

Brown, R.S., Cooke, S.J., Anderson, W.G., and McKinley, R.S. 2004. Evidence to challenge the "2% rule" for biotelemetry. N. Am. J. Fish. Manage. **19**(3): 867–871. doi:10.1577/1548-8675(1999)019<0867:etctrf>2.0.co;2.

Brownscombe, J.W., Lennox, R.J., Danylchuk, A.J., and Cooke, S.J. 2018. Estimating fish swimming metrics and metabolic rates with accelerometers: the influence of sampling frequency. J. Fish Biol. **93**(2): 207–214. doi:10.1111/jfb.13652. PMID:29931782.

Clarke, A., and Johnston, N.M. 1999. Scaling of metabolic rate with body mass and in teleost temperature fish. J. Anim. Ecol. **68**(5): 893–905. doi:10.1046/j.1365-2656.1999.00337.x.

Cook, C.L., and Coughlin, D.J. 2010. Rainbow trout *Oncorhynchus mykiss* consume less energy when swimming near obstructions. J. Fish Biol. **77**(7): 1716–1723. doi:10.1111/j.1095-8649.2010.02801.x. PMID:21078030.

Cooke, S.J., Kassler, T.W., and Philipp, D.P. 2001. Physiological performance of largemouth bass related to local adaptation and interstock hybridization: Implications for conservation and management. J. Fish Biol. **59**(sA): 248–268. doi:10.1111/j.1095-8649.2001.tb01389.x.

Cooke, S.J., Woodley, C.M., Eppard, M.B., Brown, R.S., and Nielsen, J.L. 2011. Advancing the surgical implantation of electronic tags in fish: a gap analysis and research agenda based on a review of trends in intracoelomic tagging effects studies. Rev. Fish Biol. Fish. **21**(1): 127–151. doi:10.1007/s11160-010-9193-3.

Coughlin, D.J. 2002. Aerobic muscle function during steady swimming in fish. Fish Fish. **3**(2): 63–78. doi:10.1046/j.1467-2979.2002.00069.x.

Crawley, M. J. 2013. The R book. 2nd ed. Wiley Publishing, Chichester. doi:10.1002/9781118448908.

Crowder, M.J. 1978. Beta-binomial Anova for proportions. J. R. Stat. Soc. Ser. C Appl. Stat. **27**(1): 34–37. doi:10.2307/2346223.

Currie, R.J., Bennett, W.A., and Beitinger, T.L. 1998. Critical thermal minima and maxima of three freshwater game-fish species acclimated to constant temperatures. Environ. Biol. Fishes, **51**(2): 187–200. doi:10.1023/A:1007447417546.

Daniels, M.D., and Rhoads, B.L. 2013. Spatial pattern of turbulence kinetic energy and shear stress in a meander bend with large woody debris. Riparian Veg. Fluv. Geomorphol. **8**: 87–97. doi:10.1029/008WSA07.

Deng, Z., Guensch, G.R., McKinstry, C.A., Mueller, R.P., Dauble, D.D., and Richmond, M.C. 2005. Evaluation of fish-injury mechanisms during exposure to turbulent shear flow. Can. J. Fish. Aquat. Sci. **62**(7): 1513–1522. doi:10.1139/f05-091.

Downs, P.W., and Kondolf, G.M. 2002. Post-project appraisals in adaptive management of river channel restoration. Environ. Manage. **29**(4): 477–496. doi:10.1007/s00267-001-0035-X. PMID:12071499.

Dudgeon, D., Arthington, A.H., Gessner, M.O., Kawabata, Z.-I., Knowler, D.J., Lévêque, C., et al. 2006. Freshwater biodiversity: importance, threats, status and conservation challenges. Biol. Rev. Camb. Philos. Soc. **81**(2): 163–182. doi:10.1017/S1464793105006950. PMID:16336747.

Eaton, J.G., and Scheller, R.M. 1996. Effects of climate warming on fish thermal habitat in streams of the United States. Limnol. Oceanogr. **41**(5): 1109–1115. doi:10.4319/lo.1996.41.5.1109.

Enders, E.C., and Boisclair, D. 2016. Effects of environmental fluctuations on fish metabolism: Atlantic salmon *Salmo salar* as a case study. J. Fish Biol. **88**(1): 344–358. doi:10.1111/jfb.12786. PMID:26577543.

Enders, E.C., Boisclair, D., and Roy, A.G. 2003. The effect of turbulence on the cost of swimming for juvenile Atlantic salmon (*Salmo salar*). Can. J. Fish. Aquat. Sci. **60**(9): 1149–1160. doi:10.1139/f03-101.

Ennis, D.M., and Bi, J. 1998. The beta-binomial model: accounting for inter-trial variation in replicated difference and preference tests. J. Sens. Stud. **13**(4): 389–412. doi:10.1111/j.1745-459X.1998.tb00097.x.

EPA. 2017. National Water Quality Inventory: Report to Congress. EPA 841-R-16-011 National Water Quality Inventory. United States Environmental Protection Agency, Washington, D.C.

Fausch, K.D. 1993. Experimental analysis of microhabitat selection by juvenile steelhead (*Oncorhynchus mykiss*) and coho salmon (*O. kisutch*) in a British Columbia stream. Can. J. Fish. Aquat. Sci. **50**(6): 1198–1207. doi:10.1139/f93-136.

Fox, J., and Weisberg, S. 2019. An R companion to applied regression. 3rd ed. Sage Publications, Thousand Oaks, Calif. Available from https://socialsciences.mcmaster.ca/jfox/Books/Companion/.

Gilvear, D.J., Spray, C.J., and Casas-Mulet, R. 2013. River rehabilitation for the delivery of multiple ecosystem services at the river network scale. J. Environ. Manage. **126**: 30–43. doi:10.1016/j.jenvman.2013.03.026. PMID:23659798.

Gleick, P.H. 2003. Global freshwater resources: soft-path solutions for the 21st century. Science, **302**(5650): 1524–1528. doi:10.1126/science.1089967. PMID:14645837.

Harms, C.A. 2005. Surgery in fish research: common procedures and postoperative care. Lab. Anim. **34**(1): 28–34. doi:10.1038/laban0105-28. PMID:19795589.

Hartig, F. 2019. DHARMa: residual diagnostics for hierarchical (multi-level/mixed) regression models. Available from https://cran.r-project.org/package=DHARMa.

Hocutt, C.H. 1973. Swimming performance of three warmwater fishes exposed to a rapid temperature change. Chesap. Sci. **14**(1): 11–16. doi:10.2307/1350698.

Hofmann, G.E., and Todgham, A.E. 2010. Living in the now: physiological mechanisms to tolerate a rapidly changing environment. Annu. Rev. Physiol. **72**(1): 127–145. doi:10.1146/annurev-physiol-021909-135900. PMID:20148670.

Hrodey, P.J., and Sutton, T.M. 2008. Fish community responses to half-log additions in warmwater streams. N. Am. J. Fish. Manage. **28**(1): 70–80. doi:10.1577/m06-168.1.

Jeffrey, J.D., Hasler, C.T., Chapman, J.M., Cooke, S.J., and Suski, C.D. 2015. Linking landscape-scale disturbances to stress and condition of fish: implications for restoration and conservation. Integr. Comp. Biol. **55**(4): 618–630. doi:10.1093/icb/icv022. PMID:25931612.

Jelks, H.L., Walsh, S.J., Burkhead, N.M., Contreras-Balderas, S., Díaz-Pardo, E., Hendrickson, D.A., et al. 2008. Conservation status of imperiled North American freshwater and diadromous fishes. Fisheries, **33**(8): 372–407. doi:10.1577/1548-8446-33.8.372.

Johnston, I.A., and Dunn, J. 1987. Temperature acclimation and metabolism in ectotherms with particular reference to teleost fish. Symp. Soc. Exp. Biol. **41**: 67–93. PMID:3332497.

Kail, J., Brabec, K., Poppe, M., and Januschke, K. 2015. The effect of river restoration on fish, macroinvertebrates and aquatic macrophytes: a meta-analysis. Ecol. Indic. **58**: 311–321. doi:10.1016/j.ecolind.2015.06.011.

Kern, P., Cramp, R.L., Gordos, M.A., Watson, J.R., and Franklin, C.E. 2018. Measuring U_{crit} and endurance: equipment choice influences estimates of fish swimming performance. J. Fish Biol. **92**(1): 237–247. doi:10.1111/jfb.13514. PMID:29193071.

Killen, S.S., Marras, S., Steffensen, J.F., and Mckenzie, D.J. 2012. Aerobic capacity influences the spatial position of individuals within fish schools. Proc. R. Soc. B Biol. Sci. **279**(1727): 357–364. doi:10.1098/rspb.2011.1006. PMID:21653593.

Kolok, A.S. 1991. Photoperiod alters the critical swimming speed of juvenile largemouth bass, *Micropterus salmoides*, acclimated to cold water. Copeia, **1991**(4): 1085–1090. doi:10.2307/1446103.

Lacey, R.W.J., Neary, V.S., Liao, J.C., Enders, E.C., and Tritico, H.M. 2012. The IPOS framework: linking fish swimming performance in altered flows from laboratory experiments to rivers. River Res. Appl. **28**(4): 429–443. doi:10.1002/rra.1584.

Lenth, R. 2019. emmeans: estimated marginal means, aka least-squares means. Available from https://cran.r-project.org/package=emmeans.

Lepori, F., Palm, D., Brännäs, E., and Malmqvist, B. 2005. Does restoration of structural heterogeneity in streams enhance fish and macroinvertebrate diversity? Ecol. Appl. **15**(6): 2060–2071. doi:10.1890/04-1372.

Liao, J.C. 2004. Neuromuscular control of trout swimming in a vortex street: implications for energy economy during the Karman gait. J. Exp. Biol. **207**(Pt. 20): 3495–3506. doi:10.1242/jeb.01125. PMID:15339945.

Liao, J.C. 2007. A review of fish swimming mechanics and behaviour in altered flows. Philos. Trans. R. Soc. B Biol. Sci. **362**(1487): 1973–1993. doi:10.1098/rstb.2007.2082. PMID:17472925.

Liao, J.C., Beal, D.N., Lauder, G.V., and Triantafyllou, M.S. 2003*a*. The Karman gait: novel body kinematics of rainbow trout swimming in a vortex street. J. Exp. Biol. **206**(Pt. 6): 1059–1073. doi:10.1242/jeb.00209. PMID:12582148.

Liao, J.C., Beal, D.N., Lauder, G.V., and Triantafyllou, M.S. 2003*b*. Fish exploiting vortices decrease muscle activity. Science (80-), **302**(5650): 1566–1569. doi:10.1126/science.1088295. PMID:14645849.

Louhi, P., Vehanen, T., Huusko, A., Mäki-Petäys, A., and Muotka, T. 2016. Long-term monitoring reveals the success of salmonid habitat restoration. Can. J. Fish. Aquat. Sci. **73**(12): 1733–1741. doi:10.1139/cjfas-2015-0546.

Lüdecke, D. 2019. sjstats: statistical functions for regression models. Version 0.17.5. doi:10.5281/zenodo.1284472.

Lupandin, A.I. 2005. Effect of flow turbulence on swimming speed of fish. Biol. Bull. Russ. Acad. Sci. **32**(5): 461–466. doi:10.1007/s10525-005-0125-z.

Maia, A., Sheltzer, A.P., and Tytell, E.D. 2015. Streamwise vortices destabilize swimming bluegill sunfish (*Lepomis macrochirus*). J. Exp. Biol. **218**(Pt. 5): 786–792. doi:10.1242/jeb.114363. PMID:25617456.

Manners, R.B., and Doyle, M.W. 2008. A mechanistic model of woody debris jam evolution and its application to wood-based restoration and management. River Res. Appl. **24**(8): 1104–1123. doi:10.1002/rra.1108.

McClendon, D.D., and Rabeni, C.F. 1987. Physical and biological variables useful for predicting population characteristics of smallmouth bass and rock bass in an Ozark stream. N. Am. J. Fish. Manage. **7**(1): 46–56. doi:10.1577/1548-8659(1987)7<46:pabvuf>2.0.co;2.

McMahon, T.E., and Hartman, G.F. 1989. Influence of cover complexity and current velocity on winter habitat use by juvenile coho salmon (*Oncorhynchus kisutch*). Can. J. Fish. Aquat. Sci. **46**(9): 1551–1557. doi:10.1139/f89-197.

Metcalfe, J.D., Wright, S., Tudorache, C., and Wilson, R.P. 2016. Recent advances in telemetry for estimating the energy metabolism of wild fishes. J. Fish Biol. **88**(1): 284–297. doi:10.1111/jfb.12804. PMID:26592370.

Miller, J.R., and Kochel, R.C. 2010. Assessment of channel dynamics, in-stream structures and post-project channel adjustments in North Carolina and its implications to effective stream restoration. Environ. Earth Sci. **59**(8): 1681–1692. doi:10.1007/s12665-009-0150-1.

Moerke, A.H., and Lamberti, G.A. 2003. Responses in fish community structure to restoration of two Indiana streams. N. Am. J. Fish. Manage. **23**(3): 748–759. doi:10.1577/m02-012.

Nagayama, S., and Nakamura, F. 2010. Fish habitat rehabilitation using wood in the world. Landsc. Ecol. Eng. **6**(2): 289–305. doi:10.1007/s11355-009-0092-5.

Nelson, J.A. 2016. Oxygen consumption rate v. rate of energy utilization of fishes: a comparison and brief history of the two measurements. J. Fish Biol. **88**(1): 10–25. doi:10.1111/jfb.12824. PMID:26768970.

Palmer, M.A., Hondula, K.L., and Koch, B.J. 2014. Ecological restoration of streams and rivers: shifting strategies and shifting goals. Annu. Rev. Ecol. Evol. Syst. **45**(1): 247–269. doi:10.1146/annurev-ecolsys-120213-091935.

Palmer, M.A., Menninger, H.L., and Bernhardt, E.S. 2010. River restoration, habitat heterogeneity and biodiversity: a failure of theory or practice? Freshw. Biol. **55**(Suppl. 1): 205–222. doi:10.1111/j.1365-2427.2009.02372.x.

56

Can. J. Fish. Aquat. Sci. Vol. 78, 2021

Peake, S. 2004. An evaluation of the use of critical swimming speed for determination of culvert water velocity criteria for smallmouth bass. Trans. Am. Fish. Soc. **133**(6): 1472–1479. doi:10.1577/t03-202.1.

Peake, S.J., McKinley, R.S., and Barth, C. 1997. Effect of recovery parameters on critical swimming speed of juvenile rainbow trout (*Oncorhynchus mykiss*). Can. J. Zool. **75**(10): 1724–1727. doi:10.1139/z97-800.

Pereira, G.H.A. 2019. On quantile residuals in beta regression. Commun. Stat. Simul. Comput. **48**(1): 302–316. doi:10.1080/03610918.2017.1381740.

Przybilla, A., Kunze, S., Rudert, A., Bleckmann, H., and Brücker, C. 2010. Entraining in trout: a behavioural and hydrodynamic analysis. J. Exp. Biol. **213**(Pt 17): 2976–2986. doi:10.1242/jeb.041632. PMID:20709926.

Radspinner, R.R., Diplas, P., Lightbody, A.F., and Sotiropoulos, F. 2010. River training and ecological enhancement potential using in-stream structures. J. Hydraul. Eng. **136**(12): 967–980. doi:10.1061/(ASCE)HY.1943-7900.0000260.

Rhoads, B.L., Engel, F.L., and Abad, J.D. 2011. Pool-riffle design based on geomorphological principles for naturalizing straight channels. *In* Geophysical monograph series. pp. 367–384. doi:10.1029/2010GM000979.

Ricklefs, R.E., and Wikelski, M. 2002. The physiology/life-history nexus. Trends Ecol. Evol. **17**(10): 462–468. doi:10.1016/S0169-5347(02)02578-8.

Robinson, S. 1991. Coherent motions in the turbulent boundary layer. Annu. Rev. Fluid Mech. **23**(1): 601–639. doi:10.1146/annurev.fl.23.010191.003125.

Rodgers, G.G., Tenzing, P., and Clark, T.D. 2016. Experimental methods in aquatic respirometry: the importance of mixing devices and accounting for background respiration. J. Fish Biol. **88**(1): 65–80. doi:10.1111/jfb.12848. PMID:26768972.

Rosi-Marshall, E.J., Moerke, A.H., and Lamberti, G.A. 2006. Ecological responses to trout habitat rehabilitation in a northern Michigan stream. Environ. Manage. **38**(1): 99–107. doi:10.1007/s00267-005-0177-3. PMID:16738823.

Sandblom, E., Gräns, A., Axelsson, M., and Seth, H. 2014. Temperature acclimation rate of aerobic scope and feeding metabolism in fishes: implications in a thermally extreme future. Proc. R. Soc. B Biol. Sci. **281**(1794). doi:10.1098/rspb.2014.1490.

Schneider, K.N., and Winemiller, K.O. 2008. Structural complexity of woody debris patches influences fish and macroinvertebrate species richness in a temperate floodplain-river system. Hydrobiologia, **610**(1): 235–244. doi:10.1007/s10750-008-9438-5.

Shirvell, C.S. 1990. Role of instream rootwads as juvenile coho salmon (*Oncorhynchus kisutch*) and steelhead trout (*O. mykiss*) cover habitat under varying streamflows. Can. J. Fish. Aquat. Sci. **47**(5): 852–861. doi:10.1139/f90-098.

Shuler, S.W., Nehring, R.B., and Fausch, K.D. 1994. Diel habitat selection by brown trout in the Rio Grande River, Colorado, after placement of boulder structures. N. Am. J. Fish. Manage. **14**(1): 99–111. doi:10.1577/1548-8675(1994)014<0099:dhsbbt>2.3.co;2.

Start, D., McCauley, S., and Gilbert, B. 2018. Physiology underlies the assembly of ecological communities. Proc. Natl. Acad. Sci. U.S.A. **115**(23): 6016–6021. doi:10.1073/pnas.1802091115. PMID:29784774.

Steffensen, J.F., Johansen, K., and Bushnell, P.G. 1984. An automated swimming respirometer. Comp. Biochem. Physiol. Part A Physiol. **79**(3): 437–440. doi:10.1016/0300-9629(84)90541-3.

Stewart, G.B., Bayliss, H.R., Showler, D.A., Sutherland, W.J., and Pullin, A.S. 2009. Effectiveness of engineered in-stream structure mitigation measures to increase salmonid abundance: A systematic review. Ecol. Appl. **19**(4): 931–941. doi:10.1890/07-1311.1. PMID:19544735.

Suski, C.D., and Ridgway, M.S. 2009. Seasonal pattern of depth selection in smallmouth bass. J. Zool. **279**(2): 119–128. doi:10.1111/j.1469-7998.2009.00595.x.

Svendsen, M.B., Bushnell, P.G., and Steffensen, J.F. 2016. Design and setup of intermittent-flow respirometry system for aquatic organisms. J. Fish Biol. **88**(1): 26–50. doi:10.1111/jfb.12797. PMID:26603018.

Svendsen, J.C., Skov, J., Bildsoe, M., and Steffensen, J.F. 2003. Intra-school positional preference and reduced tail beat frequency in trailing positions in schooling roach under experimental conditions. J. Fish Biol. **62**(4): 834–846. doi:10.1046/j.1095-8649.2003.00068.x.

Taguchi, M., and Liao, J.C. 2011. Rainbow trout consume less oxygen in turbulence: the energetics of swimming behaviors at different speeds. J. Exp. Biol. **214**(Pt 9): 1428–1436. doi:10.1242/jeb.052027. PMID:21490251.

Tews, J., Brose, U., Grimm, V., Tielbörger, K., Wichmann, M., Schwager, M., and Jeltsch, F. 2004. Animal species diversity driven by habitat heterogeneity/diversity: the importance of keystone structures. J. Biogeogr. **31**(1): 79–92. doi:10.1046/j.0305-0270.2003.00994.x.

Thielicke, W., and Stamhuis, E.J. 2014. PIVlab – Towards User-friendly, Affordable and Accurate Digital Particle Image Velocimetry in MATLAB. J. Open Res. Softw. **2**(1): e30. doi:10.5334/jors.bl.

Thompson, D.M. 2002. Long-term effect of instream habitat-improvement structures on channel morphology along the Blackledge and Salmon rivers, Connecticut, USA. Environ. Manage. **29**(2): 250–265. doi:10.1007/s00267-001-0069-0.

Thompson, D.M. 2005. The history of the use and effectiveness of instream structures in the United States. Rev. Eng. Geol. **16**: 35–50. doi:10.1130/2005.4016(04).

Thompson, D.M. 2006. Did the pre-1980 use of in-stream structures improve streams? A reanalysis of historical data. Ecol. Appl. **16**(2): 784–796. doi:10.1890/1051-0761(2006)016[0784:dtpuoi]2.0.co;2. PMID:16711062.

Tritico, H.M., and Cotel, A.J. 2010. The effects of turbulent eddies on the stability and critical swimming speed of creek chub (*Semotilus atromaculatus*). J. Exp. Biol. **213**(Pt. 13): 2284–2293. doi:10.1242/jeb.041806. PMID:20543127.

Tullos, D., and Walter, C. 2015. Fish use of turbulence around wood in winter: Physical experiments on hydraulic variability and habitat selection by juvenile coho salmon, *Oncorhynchus kisutch*. Environ. Biol. Fishes, **98**(5): 1339–1353. doi:10.1007/s10641-014-0362-4.

Tullos, D., Walter, C., and Dunham, J. 2016. Does resolution of flow field observation influence apparent habitat use and energy expenditure in juvenile coho salmon? Water Resour. Res. **52**(8): 5938–5950. doi:10.1002/2015WR018501.

van der Hoop, J.M., Byron, M.L., Ozolina, K., Miller, D.L., Johansen, J.L., Domenici, P., and Steffensen, J.F. 2018. Turbulent flow reduces oxygen consumption in the labriform swimming shiner perch, *Cymatogaster aggregata*. J. Exp. Biol. **221**(11): jeb168773. doi:10.1242/jeb.168773.

Vörösmarty, C.J., McIntyre, P.B., Gessner, M.O., Dudgeon, D., Prusevich, A., Green, P., et al. 2010. Global threats to human water security and river biodiversity. Nature, **467**(7315): 555–561. doi:10.1038/nature09440. PMID:20882010.

Wade, R.J., Rhoads, B.L., Rodríguez, J., Daniels, M.D., Wilson, D., Herricks, E.E., et al. 2002. Integrating science and technology to support stream naturalization near Chicago, Illinois. J. Am. Water Resour. Assoc. **38**(4): 931–944. doi:10.1111/j.1752-1688.2002.tb05535.x.

Wagner, G.N., Cooke, S.J., Brown, R.S., and Deters, K.A. 2011. Surgical implantation techniques for electronic tags in fish. Rev. Fish Biol. Fish. **21**(1): 71–81. doi:10.1007/s11160-010-9191-5.

Warhaft, Z. 2002. Turbulence in nature and in the laboratory. Proc. Natl. Acad. Sci. **99**(Suppl. 1): 2481–2486. doi:10.1073/pnas.012580299.

Webb, P.W. 1971. The swimming energetics of trout II. Oxygen consumption and swimming efficiency. J. Exp. Biol. **55**(2): 521–540. PMID:5114038.

Webb, P.W. 1998. Entrainment by river chub *Nocomis micropogon* and smallmouth bass *Micropterus dolomieu* on cylinders. J. Exp. Biol. **201**: 2403–2412. Available from https://jeb.biologists.org/content/jexbio/201/16/2403.full.pdf [accessed 14 June 2019].

Wehrly, K.E., Wiley, M.J., and Seelbach, P.W. 2003. Classifying regional variation in thermal regime based on stream fish community patterns. Trans. Am. Fish. Soc. **132**(1): 18–38. doi:10.1577/1548-8659(2003)132<0018:crvitr>2.0.co;2.

West, B.T., Welch, K.B., and Galecki, A.T. 2007. Linear mixed models: a practical guide using statistical software. *In* Statistics in medicine. Chapman & Hall/CRC, Boca Raton, Fla. doi:10.1002/sim.3167.

Wickham, H. 2016. ggplot2: Elegant graphics for data analysis. Springer-Verlag, New York.

Wilke, C.O. 2019. cowplot: streamlined plot theme and plot annotations for "ggplot2". Available from https://cran.r-project.org/package=cowplot.

Wilkes, M.A., Enders, E.C., Silva, A.T., Acreman, M., and Maddock, I. 2017. Position choice and swimming costs of juvenile Atlantic salmon *Salmo salar* in turbulent flow. J. Ecohydraulics, **2**(1): 16–27. doi:10.1080/24705357.2017.1287532.

Williamson, C. 1996. Vortex dynamics in the cylinder wake. Annu. Rev. Fluid Mech. **28**(1): 477–539. doi:10.1146/annurev.fl.28.010196.002401.

Wilson, S.M., Hinch, S.G., Eliason, E.J., Farrell, A.P., and Cooke, S.J. 2013. Calibrating acoustic acceleration transmitters for estimating energy use by wild adult Pacific salmon. Comp. Biochem. Physiol. A Mol. Integr. Physiol. **164**(3): 491–498. doi:10.1016/j.cbpa.2012.12.002.

Wohl, E., Angermeier, P.L., Bledsoe, B.P., Kondolf, G.M., MacDonnell, L., Merritt, D.M., et al. 2005. River restoration. Water Resour. Res. **41**(10). doi:10.1029/2005WR003985.

Wohl, E., Lane, S.N., and Wilcox, A.C. 2015. The science and practice of river restoration. Water Resour. Res. **51**(8): 5974–5997. doi:10.1002/2014WR016874.Received.

Ydesen, K.S., Wisniewska, D.M., Hansen, J.D., Beedholm, K., Johnson, M., and Madsen, P.T. 2014. What a jerk: prey engulfment revealed by high-rate, super-cranial accelerometry on a harbour seal (*Phoca vitulina*). J. Exp. Biol. **217**(Pt. 13): 2239–2243. doi:10.1242/jeb.100016. PMID:24737765.

Young, J.L., Bornik, Z.B., Marcotte, M.L., Charlie, K.N., Wagner, G.N., Hinch, S.G., and Cooke, S.J. 2006. Integrating physiology and life history to improve fisheries management and conservation. Fish Fish. **7**(4): 262–283. doi:10.1111/j.1467-2979.2006.00225.x.

Zhang, D. 2018. rsq: R-squared and related measures. Available from https://cran.r-project.org/package=rsq.

Zuur, A.F., Ieno, E.N., Walker, N.J., Saveliev, A.A., and Smith, G.M. 2009. Mixed effects models and extensions in ecology with R. Springer, New York. doi:10.1016/B978-0-12-387667-6.00013-0.